Supplementary Materials for

Expanding the fluorine chemistry of living systems using engineered polyketide synthase pathways

Mark C. Walker,[†] Benjamin W. Thuronyi,[†] Louise K. Charkoudian, Brian Lowry, Chaitan Khosla, and Michelle C. Y. Chang*

* Corresponding author. E-mail: mcchang@berkeley.edu

This PDF file includes:

Table of Contents

Materials and Methods

Supplementary Results

Materials and Methods

Commercial materials. Luria-Bertani (LB) Broth Miller, LB Agar Miller, Terrific Broth (TB), yeast extract, malt extract, glycerol, and triethylamine (TEA) were purchased from EMD Biosciences (Darmstadt, Germany). Carbenicillin (Cb), isopropyl-β-D-thiogalactopyranoside (IPTG), phenylmethanesulfonyl fluoride (PMSF), tris(hydroxymethyl)aminomethane hydrochloride (Tris-HCl), sodium chloride, dithiothreitol (DTT), 4-(2-hydroxyethyl)-1-piperazineethanesulfonic acid (HEPES), magnesium chloride hexahydrate, kanamycin (Km), acetonitrile, N,O-bis(trimethylsilyl)trifluoroacetamide (BSTFA), dichloromethane, ethyl acetate and ethylene diamine tetraacetic acid disodium dihydrate (EDTA), were purchased from Fisher Scientific (Pittsburgh, PA). Sodium fluoroacetate, coenzyme A trilithium salt (CoA), acetyl-CoA, malonyl-CoA, methylmalonyl-CoA, diethylfluoromalonate, malonic acid, methylmalonic acid, tris(2-carboxyethyl)phosphine (TCEP) hydrochloride, lithium hexamethyldisilazide solution (LiHMDS), phosphoenolpyruvate (PEP), adenosine triphosphate sodium salt (ATP), nicotinamide adenine dinucleotide reduced form dipotassium salt (NADH), nicotinamide adenine dinucleotide phosphate reduced form (NADPH), myokinase, pyruvate kinase, lactate dehydrogenase, poly(ethyleneimine) solution (PEI), 5-fluorouracil, β-mercaptoethanol, sodium phosphate dibasic hepthydrate, chlorotrifluoromethane and N,N,N',N'-tetramethyl-ethane-1,2-diamine (TEMED) were purchased from Sigma-Aldrich (St. Louis, MO). Formic acid was purchased from Acros Organics (Morris Plains, NJ). Acrylamide/Bis-acrylamide (30%, 37.5:1), electrophoresis grade sodium dodecyl sulfate (SDS), Bio-Rad protein assay dye reagent concentrate and ammonium persulfate were purchased from Bio-Rad Laboratories (Hercules, CA). Restriction enzymes, T4 DNA ligase, Antarctic phosphatase, Phusion DNA polymerase, T5 exonuclease, and Taq DNA ligase were purchased from New England Biolabs (Ipswich, MA). Deoxynucleotides (dNTPs) and Platinum Taq High-Fidelity polymerase (Pt Taq HF) were purchased from Invitrogen (Carlsbad, CA). PageRuler™ Plus prestained protein ladder was purchased from Fermentas (Glen Burnie, Maryland). Oligonucleotides were purchased from Integrated DNA Technologies (Coralville, IA), resuspended at a stock concentration of 100 μM in 10 mM Tris-HCl, pH 8.5, and stored at either 4°C for immediate use or -20°C for longer term use. DNA purification kits and Ni-NTA agarose were purchased from Qiagen (Valencia, CA). Complete EDTA-free protease inhibitor was purchased from Roche Applied Science (Penzberg, Germany). O-(7-Azabenzotriazol-1-yl)-N,N,N′,N′-tetramethyluronium hexafluorophosphate (HATU), Amicon Ultra 3,000 MWCO and 30,000 MWCO centrifugal concentrators, 5,000 MWCO regenerated cellulose ultrafiltration membranes, and LiChroCART 250-4 Purospher RP-18e HPLC column were purchased from EMD Millipore (Billerica, MA). Deuterium oxide and chloroform-d were purchased from Cambridge Isotope Laboratories (Andover, MA). ^{19}F NMR

spectra were collected at 25ºC on Bruker AVQ-400 or AV-600 spectrometers at the College of Chemistry NMR Facility at the University of California, Berkeley or on a Bruker Biospin 900 MHz spectrometer at the QB3 Central California 900 MHz NMR Facility or on a Bruker AV-600 spectrometer equipped with a QCI-CryoProbe at Novartis Institutes for Biomedical Research (Emeryville, California). Spectra were referenced to $CFCl_3$ (0 ppm) or 5-fluorouracil (D_2O: -168.33 ppm vs. $CFCl_3$). NMR assignments were made based on COSY, ^{13}C-^{1}H HSQC, ^{13}C-^{1}H HMBC and ^{19}F-^{1}H HMBC spectra where appropriate. High-resolution mass spectral analyses were carried out at the College of Chemistry Mass Spectrometry Facility.

Bacterial strains. *E. coli* DH10B-T1^{R} and BL21(de3)T1^{R} were used for DNA construction and heterologous protein production, respectively, except for DEBS modules, which were heterologously expressed in *E. coli* BAP1 (*45*).

Gene and plasmid construction. Standard molecular biology techniques were used to carry out plasmid construction. All PCR amplifications were carried out with Phusion or Platinum Taq High Fidelity DNA polymerases. For amplification of GC-rich sequences from *S. coelicolor*, PCR reactions were supplemented with DMSO (5%) using the standard buffer rather than GC buffer with primer annealing temperatures 8-10°C below the T_m. All constructs were verified by sequencing (Quintara Biosciences; Berkeley, CA).

The synthetic gene encoding NphT7 was optimized for *E. coli* class II codon usage and synthesized using PCR assembly (*Table S1*). Gene2Oligo was used to convert the gene sequence into primer sets using default optimization settings (*Table S1*) (*46*). To assemble the synthetic gene, each primer was added at a final concentration of 1 μM to the first PCR reaction (50 μL) containing 1 × Pt Taq HF buffer (20 mM Tris-HCl, 50 mM KCl, pH 8.4), $MgSO_4$ (1.5 mM), dNTPs (250 μM each), and Pt Taq HF (5 U). The following thermocycler program was used for the first assembly reaction: 95^{o}C for 5 min; 95^{o}C for 30 s; 55^{o}C for 2 min; 72^{o}C for 10 s; 40 cycles of 95^{o}C for 15 s, 55^{o}C for 30 s, 72^{o}C for 20 s plus 3 s/cycle; these cycles were followed by a final incubation at 72^{o}C for 5 min. The second assembly reaction (50 μL) contained 16 μL of the unpurified first PCR reaction with standard reagents for Pt Taq HF. The thermocycler program for the second PCR was: 95^{o}C for 30 s; 55^{o}C for 2 min; 72^{o}C for 10 s; 40 cycles of 95^{o}C for 15 s, 55^{o}C for 30 s, 72^{o}C for 80 s; these cycles were followed by a final incubation at 72^{o}C for 5 min. The second PCR reaction (16 μL) was transferred again into fresh reagents and run using the same program. Following gene construction, the DNA smear at the appropriate size was gel purified and used as a template for the rescue PCR (50 μL) with Pt Taq HF and rescue primers under standard conditions. The resulting rescue product was inserted into pBAD33 and

confirmed by sequencing, then amplified using the nphT7 F1/R1 primer set (*Table S1*) and inserted into the NdeI site of pET-16b using the Gibson protocol (*47*).

pET16b-His_{10}-AckA.EC and pET16b-His_{10}-Pta.EC were constructed by amplification from pRSFDuet-ackA.pta using the AckA.EC F/R and Pta.EC F/R primer sets (*Table S1*) and insertion into the NdeI-XhoI (Pta, Gene ID 12872491) or NdeI-BamHI (AckA, Gene ID 12874027) sites of pET16b. pET28a-His_6-MatB.SCo and pET28a-His_6-Epi.SCo were constructed by amplification from *S. coelicolor* A3(2) M145 (ATCC BAA-471) genomic DNA using the MatB.SCo F/R and epi.SCo F/R primer sets (*Table S1*) and insertion into the NdeI-XhoI sites of pET28a. pET16x-His_{10}-THNS was constructed by amplification out of *S. coelicolor* genomic DNA using the THNS F/R primer set (*Table S1*) and insertion into the NdeI-SpeI sites of pET16x. pCDFDuet-DszsAT.SCe-MatB.SCo and pCDFDuet-ø-MatB.SCo were constructed by amplification from pET28a-His_6-MatB.SCo and pFW3 (*40*) using the pCDF-MatB.SCo F/R and pCDF-DszsAT.SCe F/R primer sets (*Table S1*) and insertion of DszsAT.SCe and MatB.SCo into the NcoI-HindIII and NdeI-KpnI sites of pCDFDuet-1 respectively. pTRC33-NphT7-PhaB was constructed by amplifying NphT7 from pET-16b-NphT7 using the NphT7 G F/G R primer set (*Table S1*) and PhaB from pBT33-PhaABC (*48*) using the PhaB F/R primer set (*Table S1*) where each forward primer included the RBS from pET16b, then inserting both genes simultaneously into the BamHI-XbaI sites of pTRC33 using the Gibson protocol. pSV272-His_6-MBP-$DEBS_{Mod2}$ and pSV272-His_6-MBP-$DEBS_{Mod2}/AT^0$ (S2652A based on EryAI numbering) were constructed by amplification from pBP19 (*42*) using the MBP-M2 F/R primer set (pSV272-MBP-$DEBS_{Mod2}$-His_6) (*Table S1*) or MBP-M2 F/MBP-M2ATnull R and MBP-M2ATnull F/MBP-M2 R (pSV272-MBP-$DEBS_{Mod2}/AT^0$-His_6) (*Table S1*) and insertion into the SfoI-HindIII sites of pSV272.1 using the Gibson protocol. pBAD33.BirA.EC was cloned by the QB3 Macrolab.

Expression of His-tagged proteins. TB (1 L) containing carbenicillin, kanamycin, and chloramphenicol (50 μg/mL) as appropriate in a 2.8 L Fernbach baffled shake flask was inoculated to OD_{600} = 0.05 with an overnight TB culture of freshly transformed *E. coli* containing the appropriate overexpression plasmid. The cultures were grown at 37°C at 250 rpm to OD_{600} = 0.6 to 0.8 at which point cultures were cooled on ice for 20 min, followed by induction of protein expression with IPTG (His_{10}-AckA, His_{10}-Pta: 1 mM; His_{10}-AccA/B/C/D, His_{10}-THNS, $DEBS_{Mod6}/AT^0$+TE-His_6 [pAYC138, (*40*)]: 0.4 mM; His_6-MatB, His_6-Epi, His_{10}-NphT7, DszsAT-His_6[pFW3, (*40*)], $DEBS_{Mod6}$+TE-His_6[pRSG54, (*36*)], $DEBS_{Mod3}$+TE-His_6[pRSG34, (*35*)], $DEBS_{Mod3}/AT^0$+TE-His_6[pAYC136, (*40*)], MBP-$DEBS_{Mod2}$-His_6, MBP-$DEBS_{Mod2}/AT^0$-His_6: 0.2 mM) and overnight growth at 16°C. For His_{10}-AccB expression, pBAD33-BirA was co-expressed (L-arabinose, 0.2 %) and the medium was supplemented with

20 nM D-(+)-biotin at induction. For MBP-DEBS$_{Mod2}$-His$_6$ and MBP-DEBS$_{Mod2}$/AT^0-His$_6$, pRARE2 was co-expressed. Cell pellets were harvested by centrifugation at 9,800 × *g* for 7 min at 4ºC and stored at -80ºC.

Purification of His$_{10}$-AckA, His$_{10}$-Pta, His$_6$-MatB, His$_6$-Epi, His$_{10}$-AccA/B/C/D, DszsAT-His$_6$ and His$_{10}$-NphT7. Frozen cell pellets were thawed and resuspended at 5 mL/g cell paste with Buffer A (50 mM sodium phosphate, 300 mM sodium chloride, 20% glycerol, 20 mM BME, pH 7.5) containing imidazole (10 mM) for His$_{10}$-AckA, His$_{10}$-Pta, His$_{10}$-AccA/B/C/D, His$_{10}$-NphT7, and DszsAT-His$_6$ or Buffer B (200 mM sodium phosphate, 200 mM sodium chloride, 30% glycerol, 2.5 mM EDTA, 2.5 mM DTT, pH 7.5) for His$_6$-MatB and His$_6$-Epi. Complete EDTA-free protease inhibitor cocktail (Roche) was added to the lysis buffer before resuspension. The cell paste was homogenized before lysis by passage through a French Pressure cell (Thermo Scientific; Waltham, MA) at 14,000 psi. The lysate was centrifuged at 15,300 × *g* for 20 min at 4°C to separate the soluble and insoluble fractions. DNA was precipitated in the soluble fraction by addition of 0.15% (w/v) poly(ethyleneimine). The precipitated DNA was removed by centrifugation at 15,300 × *g* for 20 min at 4°C. The remaining soluble lysate was diluted three-fold with Buffer A containing imidazole (10 mM) and loaded onto a Ni-NTA agarose column (Qiagen, 1 mL resin/g cell paste) by gravity flow or on an ÄKTApurifier FPLC (2 mL/min; GE Healthcare; Piscataway, NJ). The column was washed with Buffer A until the eluate reached an $A_{280\ nm} < 0.05$ or was negative for protein content by Bradford assay (Bio-Rad).

His$_{10}$-AckA, His$_{10}$-Pta, His$_6$-MatB, His$_{10}$-AccB, His$_{10}$-AccD, and DszsAT-His$_6$. The column was washed with 5 to 10 column volumes with Buffer A supplemented with imidazole (His$_{10}$-AckA, 40 mM; His$_{10}$-Pta, 35 mM; His$_6$-MatB, His$_{10}$-AccB, His$_{10}$-AccD, and DszsAT-His$_6$, 20 mM). The protein was then eluted with 300 mM imidazole in Buffer A.

His$_6$-Epi. His$_6$-Epi was eluted using a linear gradient from 0 to 300 mM imidazole in Buffer A over 30 column volumes.

His$_{10}$-AccA, His$_{10}$-AccC and His$_{10}$-NphT7. The column was washed with a linear gradient from 10 to 90 mM imidazole in Buffer A over 15 column volumes and then eluted with 300 mM imidazole in Buffer A.

Fractions containing the target protein were pooled by $A_{280\ nm}$ and concentrated using either an Amicon Ultra spin concentrator (3 kDa MWCO, Millipore) or an Amicon ultrafiltration cell under nitrogen flow (65 psi) using a membrane with an appropriate nominal molecular weight

cutoff (Ultracel-5 or YM10, Millipore). Protein was then exchanged into Buffer C (50 mM HEPES, 100 mM sodium chloride, 2.5 mM EDTA, 20% glycerol, pH 7.5) with (His_{10}-AckA, His_{10}-Pta, His_{10}-AccA/B/C/D, His_{10}-NphT7, DszsAT-His_6) or without (His_6-MatB and His_6-Epi) DTT (0.5-1 mM) using a Sephadex G-25 column (Sigma-Aldrich, bead size 50-150 μm, 10 mL resin/mL protein solution), then concentrated again before storage.

Final protein concentrations before storage were estimated using the $\varepsilon_{280\ nm}$ calculated by ExPASY ProtParam as follows: His_{10}-AckA: 14.8 mg/mL ($\varepsilon_{280\ nm}$ = 24,860 M^{-1} cm^{-1}), His_{10}-Pta: 16.5 mg/mL ($\varepsilon_{280\ nm}$ = 37,360 M^{-1} cm^{-1}), His_6-MatB: 19.8 mg/mL ($\varepsilon_{280\ nm}$ = 33,920 M^{-1} cm^{-1}), His_6-Epi: 18.5 mg/mL ($\varepsilon_{280\ nm}$ = 11,460 M^{-1} cm^{-1}), His_{10}-AccA: 33.2 mg/mL ($\varepsilon_{280\ nm}$ = 25,900 M^{-1} cm^{-1}), His_{10}-AccB: 23.0 mg/mL ($\varepsilon_{280\ nm}$ = 2,980 M^{-1} cm^{-1}), His_{10}-AccC: 32.6 mg/mL ($\varepsilon_{280\ nm}$ = 27,850 M^{-1} cm^{-1}), His_{10}-AccD: 4.5 mg/mL ($\varepsilon_{280\ nm}$ = 16,960 M^{-1} cm^{-1}), DszsAT-His_6: 1.7 mg/mL ($\varepsilon_{280\ nm}$ = 17,420 M^{-1} cm^{-1}), His_{10}-NphT7: 0.4 mg/mL ($\varepsilon_{280\ nm}$ = 26,930 M^{-1} cm^{-1}). All proteins were aliquoted, flash-frozen in liquid nitrogen, and stored at -80°C.

Purification of $DEBS_{Mod6}$+TE-His_6, $DEBS_{Mod6}/AT^0$+TE-His_6, $DEBS_{Mod3}$+TE-His_6, and $DEBS_{Mod3}/AT^0$+TE-His_6. The His-tagged DEBS module with thioesterase ($DEBS_{Mod6}$+TE) construct was heterologously expressed in *E. coli* BAP1 pRSG54 as described previously and purified using a modified literature protocol (*49*). Cleared cell lysates were prepared in Buffer B as described above, diluted three-fold with Buffer A, and passed over a Ni-NTA agarose column (Qiagen, approximately 1 mL/g cell paste) on an ÄKTApurifier FPLC. The column was washed with Buffer A until the eluate reached an $A_{280\ nm} < 0.05$. Protein was eluted with Buffer D (50 mM sodium phosphate, 50 mM sodium chloride, 20 mM BME, 20% glycerol, 100 mM imidazole, pH 7.5). The eluate was diluted three-fold with Buffer E (50 mM HEPES, 2.5 mM EDTA, 2.5 mM DTT, 20% glycerol, pH 7.5), loaded onto a HiTrap Q HP column (GE Healthcare, 5 mL), and eluted with a linear gradient from 0 to 1 M sodium chloride in Buffer E over 30 column volumes (4.5 mL/min). Fractions containing the target protein (eluted at ~350 mM sodium chloride) were pooled by $A_{280\ nm}$ and concentrated under nitrogen flow (65 psi) in an Amicon ultrafiltration cell using a YM10 membrane. The protein was flash-frozen in liquid nitrogen and stored at -80°C at a final concentration of 6-30 mg/mL, which was estimated using the calculated $\varepsilon_{280\ nm}$ ($DEBS_{Mod3}$ and $DEBS_{Mod3}/AT^0$: 203,280 $M^{-1}cm^{-1}$; $DEBS_{Mod6}$ and $DEBS_{Mod6}/AT^0$: 206,260 M^{-1} cm^{-1}).

Purification of MBP-$DEBS_{Mod2}$-His_6 and MBP-$DEBS_{Mod2}/AT^0$-His_6. Cleared lysates were prepared as described for other DEBS modules, diluted three-fold with Buffer A containing 10 mM imidazole, and bound in batch to Ni-NTA resin (2.5 mL/g cell paste) for 2 h. The slurry was

poured into a fritted column and washed with Buffer A containing 10 mM imidazole until the eluate reached $A_{280\ nm} < 0.05$. The protein was eluted with Buffer A containing 300 mM imidazole and concentrated to ~1 mg/mL in an Amicon ultrafiltration cell using a YM10 (30 kD NMWL) membrane. The protein was then dialyzed overnight against Buffer E containing 50 mM NaCl with TEV protease (1 mg/100 mg protein substrate) to remove the MBP tag. The protein was loaded onto a HiTrap Q HP column and eluted by a linear gradient from 0 to 500 mM NaCl in Buffer E over 20 column volumes. Fractions containing the desired protein were identified by SDS-PAGE (eluting at ~350 mM NaCl), pooled, and concentrated in a YM10 (30 kD NMWL) Amicon Ultra spin concentrator. Protein aliquots were flash-frozen in liquid nitrogen and stored at -80°C at a final concentration of 20-25 mg/mL, which was estimated using the calculated $\varepsilon_{280\ nm}$ (158,360 $M^{-1}cm^{-1}$).

Purification of His_{10}-THNS. His_{10}-THNS was purified according to a modified literature procedure (*31*). Cleared cell lysates were prepared in Buffer F (50 mM Tris-HCl, 500 mM sodium chloride, 20 mM BME, 10% glycerol pH 8) supplemented with imidazole (10 mM), PMSF (0.75 mM), and Tween 20 (1% v/v) as described above, diluted with Buffer G containing imidazole (10 mM) and Tween 20 (1%), and loaded onto a HisTrap FF column (GE Healthcare, 1 mL) on an ÄKTApurifier FPLC (1 mL/min). The column was washed with 10 mM followed by 20 mM imidazole in Buffer G, each time until the eluate reached an $A_{280\ nm} < 0.05$. Protein was eluted with 300 mM imidazole in Buffer G and concentrated with an Amicon Ultra spin concentrator (10 kDa MWCO). His_{10}-THNS was then exchanged into Buffer C containing DTT (1 mM) using a Sephadex G-25 column (Sigma-Aldrich, bead size 50-150 μm, 10 mL/mL protein solution) and concentrated again. The protein was flash-frozen in liquid nitrogen and stored at -80°C at a final concentration of 4.4 mg/mL, which was estimated using the calculated $\varepsilon_{280\ nm}$ (33,920 $M^{-1}\ cm^{-1}$).

ESI-MS screening method for acyl-CoAs. Preparative HPLC fractions were screened on an Agilent 1290 HPLC system using a Zorbax Eclipse Plus C-18 column (3.5 μm, 2.1 × 30 mm, Agilent) with a linear gradient from 0 to 65% acetonitrile over 2 min with 0.1% formic acid as the aqueous mobile phase (0.75 mL/min). Mass spectra were recorded on an Agilent 6130 single quadrupole MS with ESI source, operating in negative and positive ion scan mode.

Fluoromalonate. Diethylfluoromalonate (0.5 mL, 3.2 mmol) was saponified with methanolic sodium hydroxide (2 M, 3.5 mL) in dichloromethane and methanol (9:1 v/v, 32 mL) and the sodium salt isolated by filtration through a Büchner funnel with a fine porosity glass frit (*50*). **^{19}F NMR** (565 MHz, D_2O, 5-fluorouracil = -168.3 ppm): δ -176.43 (d, J=53 Hz).

Fluoromalonyl-CoA. Fluoromalonyl-CoA was prepared enzymatically from fluoromalonate and CoA using MatB and ATP. A myokinase/pyruvate kinase/PEP system was also used to regenerate ATP in order to avoid high concentrations of AMP that might inhibit MatB. The reaction mixture (10 mL) contained 100 mM sodium phosphate, pH 7.5, phosphoenolpyruvate (5 mM), TCEP (2.5 mM), magnesium chloride (5 mM), fluoromalonate (2.5 mM), ATP (2.5 mM), pyruvate kinase (36 U), myokinase (20 U), CoA (2 mM) and MatB (5 μM). The mixture was incubated at 37°C for 6 h and then at room temperature for 16 h before lyophilizing overnight. The residue was dissolved in water (1.6 mL) and acidified to pH ~2 by addition of 70% perchloric acid (160 μL). Insoluble material was removed by centrifugation at 18,000 × *g* for 10 min. The supernatant was adjusted to pH 6 by addition of 10 M sodium hydroxide (100 μL) and desalted on an Agilent 1200 HPLC system using a Zorbax Eclipse XDB C-18 column (5 μm, 9.4 × 250 mm, Agilent) with a linear gradient from 0 to 10% methanol over 9 min with 50 mM sodium phosphate, 25 mM trifluoroacetic acid, pH 4.5 as the aqueous mobile phase (3 mL/min). Fractions eluting near the void volume, containing both fluoromalonyl-CoA and CoA, were lyophilized overnight, dissolved in water (1 mL), and purified using a Zorbax Eclipse XDB C-18 column (5 μm, 9.4 × 250 mm) with a linear gradient from 0 to 50% methanol over 45 min with 50 mM sodium phosphate, pH 4.5 as the aqueous mobile phase (3 mL/min). Fractions were screened by ESI-MS and those containing pure fluoromalonyl-CoA were lyophilized overnight, dissolved in water (1 mL), and desalted using a Zorbax Eclipse XDB C-18 column (5 μm, 9.4 × 250 mm) with a linear gradient from 0 to 15% acetonitrile over 30 min with water as the mobile phase (3 mL/min). The desalted fluoromalonyl-CoA was lyophilized and redissolved in water or D_2O. The fluoromalonyl-CoA solutions were stored at -20°C but are stable for at least 24 h at room temperature. During NMR measurements in D_2O, complete H-D exchange occurred at the fluorine-substituted carbon over the course of 48 h. Spectra are shown in Figure S4. **^{1}H NMR** (600 MHz, D_2O, MeOH = 3.34 ppm)**:** δ 8.55 (s, 1H, H_8), 8.27 (s, 1H, H_2), 6.17 (d, J=6.6 Hz, 1H, $H_{1'}$), 5.23 (d, J=50.3 Hz, 1H, O_2C-C<u>H</u>F-C=O), 4.89 – 4.79 (m, 2H, $H_{2'}$ and $H_{3'}$), 4.59 (m, 1H, $H_{4'}$), 4.23 (m, 2H, $H_{5'}$), 4.00 (s, 1H, $H_{3''}$), 3.82 (dd, J=10.2, 4.6 Hz, 1H, pro-R-$H_{1''}$), 3.54 (dd, J=10.0, 4.4 Hz, 1H, pro-S- $H_{1''}$), 3.49 – 3.39 (m, 2H, $H_{5''}$), 3.38 – 3.29 (m, 2H, $H_{8''}$), 3.11-3.02 (m, 2H, $H_{9''}$), 2.42 (t, J=6.7 Hz, 3H, $H_{6''}$), 0.88 (s, 3H, $H_{10''}$), 0.74 (s, 3H, $H_{11''}$). **^{13}C NMR** (226 MHz, D_2O, CH_3OH = 49.15 ppm)**:** δ 196.92, 196.85 (d, J=27.5 Hz, <u>C</u>O_2), 175.02 ($C_{4''}$), 174.32 ($C_{7''}$), 169.52 (d, J=21.0 Hz, O_2C-CDF-<u>C</u>=O), 155.37 (C_6), 152.40 (C_2), 149.57 (C_4), 140.37 (C_8), 118.91 (C_5), 93.32 (td, J=25 Hz, 197 Hz, O_2C-<u>C</u>DF-C=O), 86.61 ($C_{1'}$), 83.81 (d, J=9 Hz, $C_{4'}$), 74.56 (d, J=5 Hz, $C_{3'}$ or $C_{1''}$), 74.35 ($C_{3''}$), 74.00 (d, J=5 Hz, $C_{2'}$), 72.16 (d, J=6 Hz, $C_{3'}$ or $C_{1''}$), 65.56 ($C_{5'}$), 38.66 ($C_{5''}$ or $C_{6''}$), 38.58 (d, J=8 Hz, $C_{8''}$) 35.58 (d, J=30 Hz, $C_{9''}$), 27.60 (d, J=3 Hz, $C_{5''}$ or $C_{6''}$), 21.16 ($C_{10''}$), 18.22 ($C_{11''}$). **^{19}F NMR** (565 MHz, D_2O, CF_3CO_2H = -76.20 ppm)**:** δ -

182.11 (dd, J=7.8, 50.4 Hz, O_2C-CHF-C=O), -182.72 (m, O_2C-CDF-C=O). **HR-ESI-MS [M-H]$^-$:** calculated for $C_{24}H_{36}FN_7O_{19}P_3S$**,** *m/z*, 870.0989, found *m/z* 870.0991.

Enzyme assays. Kinetic parameters (k_{cat}, K_M) were determined by fitting the data using Microcal Origin to the equation: $v_o = v_{max}$ [S] / (K_M + [S]), where v is the initial rate and [S] is the substrate concentration. Data are reported as mean ± s.e. (n = 3) unless otherwise noted with standard error derived from the nonlinear curve fitting. Error bars on graphs represent mean ± s.d. (n = 3). Error in k_{cat}/K_M is calculated by propagation of error from the individual kinetic parameters.

Acetyl-CoA carboxylase. ACCase activity was measured using a discontinuous HPLC assay. Assays were performed at 30°C in a total volume of 200 µL containing 50 mM HEPES, pH 7.5, TCEP (10 mM), bovine serum albumin (3 mg/mL), CoA (0.5 mM), ATP (2.5 mM), magnesium chloride (10 mM), sodium bicarbonate (75 mM), acetate or fluoroacetate (10 mM), phosphoenolpyruvate (10 mM), pyruvate kinase (4 U), AckA (0.1 µM), Pta (10 µM) and ACCase (15 µM). The pH of the buffer remained unchanged after addition of sodium bicarbonate. ACCase stock solution was prepared by pre-mixing the protein subunits at equimolar ratio (85 µM) except for AccB, which was added at 1.5-fold molar excess. The reaction was initiated with addition of ATP. Aliquots (20 µL) were removed and quenched by the addition of 70% perchloric acid (1 µL). Insoluble material was removed by centrifugation and the supernatant was analyzed on an Agilent 1200 or 1290 HPLC system on a LiChroCART 250-4 Purospher RP-18e column (5 µm, 4.6 × 250 mm, Millipore) and monitored at $A_{260\ nm}$. For reactions with acetate, a linear gradient from 2 to 20% acetonitrile over 10 min with 5 mM sodium phosphate and 5 mM sodium citrate with 0.1% trifluoroacetic acid, pH 4.6 as the aqueous mobile phase (1 mL/min) was used to analyze the reaction. For reactions with fluoroacetate, a linear gradient from 2 to 15% acetonitrile containing 0.1% TEA over 15 min with 10 mM Tris, pH 8.0 containing 0.1% TEA as the aqueous mobile phase (1 mL/min) was used. Buffers containing TEA were made fresh daily and could be used for at least 6 h before significant change in chromatography was observed.

Malonyl-CoA synthetase. MatB activity was measured using a modified literature method (*51*). The production of AMP was coupled to pyruvate formation by myokinase and pyruvate kinase, which in turn was coupled to NADH oxidation by lactate dehydrogenase. Assays were performed at 30°C in a total volume of 200 µL containing 100 mM HEPES, pH 7.5, TCEP (1 mM), ATP (2.5 mM), magnesium chloride (5 mM), phosphoenolpyruvate (1 mM), NADH (0.3 mM), myokinase (0.5 U), pyruvate kinase (3.6 U), lactate dehydrogenase (2.6 U), dicarboxylic

acid (25 μM – 1 mM malonate, 50 μM – 10 mM fluoromalonate or 25 μM – 1.5 mM methylmalonate) and MatB (26 nM for malonate, 1 μM for fluoromalonate and 200 nM for methylmalonate). The reaction was initiated with addition of CoA (0.5 mM) and monitored at 340 nm in a Beckman Coulter DU-800 spectrophotometer.

Acetoacetyl-CoA synthase. NphT7 activity was measured using a NADPH-coupled assay with PhaB. Assays were performed at 30°C in a total volume of 500 μL containing 50 mM HEPES, pH 7.5, NADPH (160 μM), acetyl-CoA (200 μM), PhaB (0.05 mg/mL), NphT7 (0.2 μM for malonyl-CoA; 0.5μM for fluoromalonyl-CoA) and malonyl-CoA (5 – 150 μM) or fluoromalonyl-CoA (5 – 200 μM). Reactions were initiated with the addition of malonyl- or fluoromalonyl-CoA and monitored at 340 nm in an Agilent 8453 diode array spectrophotometer. The PhaB-coupled assay was tested both by doubling NphT7, which doubled the initial velocity with both the fluorinated and non-fluorinated substrates, and also by doubling the amount of PhaB, which led to no difference in initial velocity.

Acyl-CoA hydrolysis by DEBS. Hydrolytic activity of $DEBS_{Mod6}$+TE was measured by monitoring the reaction of free CoA with DTNB as described previously (*52*). Assays were performed at 37°C in a total volume of 200 μL containing 400 mM sodium phosphate, pH 7.5, 500 μM DTNB, and $DEBS_{Mod6}$+TE (1 μM). Reactions were initiated by addition of acyl-CoA (0.5 mM) and monitored at 412 nm in a Beckman Coulter DU-800 spectrophotometer. Release of CoA was quantified by comparison to a standard curve (5–100 μM).

Tetrahydroxynaphthalene synthase. THNS activity was measured by monitoring THN production spectrophotometrically at 340 nm as previously described (*31*). The specific activity was comparable to the reported value.

Tetrahydroxynaphthalene production using THNS. All reactions (160 μL) contained 100 mM HEPES, pH 7.5, magnesium chloride (10 mM), BSA (300 μg/mL), sodium bicarbonate (75 mM), phosphoenolpyruvate (10 mM) and pyruvate kinase (2.9 U). The following final concentrations of substrates and enzymes were added to the appropriate reactions: AckA (10 nM), Pta (10 μM), ACCase (5 μM), MatB (5 μM), myokinase (1.6 U), sodium malonate (5 mM), malonyl-CoA (0.5 mM), acetyl-CoA (0.5 mM), and ATP (2.5 mM). ACCase was incubated at 30°C for 10 min with the reaction mixture before initiation with THNS (2.5 μM). When AckA/Pta activation of acetate was included, reaction mixtures were pre-incubated at 30°C for 6 min before addition of ACCase. Reactions containing TCEP (2.5 mM) were also tested, but no apparent effect on THN production was observed. All reactions were incubated at 30°C for 24 h

and flash-frozen in liquid nitrogen. Samples were thawed individually on ice before quantifying total polyketide production using a Beckman DU-800 spectrophotometer. $A_{510\ nm}$ was taken as a measure of tetrahydroxynaphthalene, flaviolin, and their spontaneous polymerization products (*53*).

2-fluoro-3-hydroxybutyryl-CoA production using NphT7. As acetofluoroacetyl-CoA proved to degrade fairly rapidly under the assay conditions, 2-fluoro-3-hydroxybutyryl-CoA was isolated from a 10 mL reaction containing 100 mM HEPES, pH 7.5, fluoromalonate (10 mM), CoA (500 μM), NADPH (1 mM), ATP (1 mM), magnesium chloride (5 mM), phosphoenolpyruvate (10 mM), pyruvate kinase (180 U), myokinase (100 U), MatB (40 μM), PhaB (7 μM) and NphT7 (2 μM) that was initiated by the addition of acetyl-CoA (0.5 mM, limiting reagent). The reaction was incubated at 30°C overnight followed by quenching by the addition of 70% perchloric acid (50 μL). 2-fluoro-3-hydroxybutryl-CoA was purified using a Zorbax Eclipse XDB C-8 column (5 μm, 9.4 × 250 mm, Agilent) with a linear gradient from 0 to 5% acetonitrile over 30 min (3 mL/min) with 50 mM sodium phosphate with 0.1% trifluoroacetic acid (pH 4.5) as the aqueous mobile phase. Fractions containing 2-fluoro-3-hydroxybutryl-CoA were identified by ESI-MS and lyophilized. The remaining solid was dissolved in water (1 mL) and purified a second time a Zorbax Eclipse XDB C-8 column (5 μm, 9.4 × 250 mm, Agilent) with a linear gradient from 0 to 5% acetonitrile over 30 min (3 mL/min) with 0.1% formic acid as the aqueous mobile phase. Fractions containing 2-fluoro-3-hydroxybutryl-CoA were identified by ESI-MS and lyophilized. Two diastereomers were observed by NMR in an approximately 2.5:1 ratio. **^{1}H NMR** (600 MHz, D_2O, acetonitrile = 2.06 ppm)**:** δ 8.54 (s, 1H, H_8), 8.30 (s, 1H, H_2), 6.08 (d, J=5.9 Hz, 1H, $H_{1'}$), 4.93 (dd, J=47.8, 2.6 Hz, 0.2H, HOCH-C<u>H</u>F-C=O minor diastereomer), 4.85 (dd, J=46.9, 2.2 Hz, 0.8H, HOCH-C<u>H</u>F-C=O major diastereomer), 4.77 – 4.77 (m, 2H, $H_{2'}$ and $H_{3'}$), 4.46 (m, 1H, $H_{4'}$), 4.16-4.04 (m, 3H, HOC<u>H</u>-CHF-C=O, $H_{5'}$), 3.89 (s, 1H, $H_{3''}$), 3.72 (d, J=7.1 Hz, 1H, $H_{1''}$ *pro-R*), 3.46 (d, J=9.7 Hz, 1H, pro-S- $H_{1''}$ *pro-S*), 3.31 (t, J=6.5 Hz, 2H, $H_{5''}$), 3.26 – 3.20 (m, 2H, $H_{8''}$), 2.95 (m, 2H, $H_{9''}$), 2.30 (t, J=6.5 Hz, 2H, $H_{6''}$), 1.15 (d, J=6.7 Hz, 2H, <u>H</u>$_3$C-HOCH-CHF major diastereomer), 1.05 (d, J=6.4 Hz, 1H, <u>H</u>$_3$C-HOCH-CHF minor diastereomer), 0.79 (s, 3H, $H_{10''}$), 0.67 (s, 3H, $H_{11''}$). **^{19}F NMR** (565 MHz, D_2O, CF_3CO_2H = -76.20 ppm)**:** δ -198.62 (dd, J=48.24, 23.3 Hz, HOCH-CH<u>F</u>-C=O), -206.85 (dd, J=46.9, 27.5, HOCH-CH<u>F</u>-C=O). **ESI-MS [M+H]$^+$:** calculated for $C_{25}H_{42}FN_7O_{18}P_3S$**,** *m/z*, 872.2, found *m/z* 872.0.

Triketide lactone production using DEBS$_{Mod6}$+TE and MatB. Assay and preparative mixtures contained 400 mM sodium phosphate, pH 7.5, phosphoenolpyruvate (50 mM), TCEP (5 mM), magnesium chloride (10 mM), ATP (2.5 mM), pyruvate kinase (27 U/mL), myokinase (10

U/mL), CoA (0.5 mM), methylmalonyl-CoA epimerase (5 μM), MatB (40 μM or as specified) and fluoro- or methylmalonate (10 – 20 mM). Including NADPH resulted in only trace yields of reduced triketide product, even with the native methylmalonyl-CoA extender, so the cofactor was omitted. This mixture was incubated at 37°C for 30-45 min and then initiated by addition of the N-acetylcysteamine thioester of (2*S*,3*R*)-2-methyl-3-hydroxypentanoic acid (NDK-SNAC, 1 – 10 mM) (*54*) and $DEBS_{Mod6}$+TE (10 μM). Aliquots (35 μL) were removed and quenched by addition of 70% perchloric acid (1.75 μL). Samples were centrifuged at 18,000 × *g* to pellet the precipitated protein. The supernatant (33 μL) was removed and added to 1 M sodium bicarbonate (6.6 μL) bringing the final pH to 4-5. Excess salts were precipitated by freezing in liquid nitrogen and centrifuging at 18,000 × *g* until thawed. The supernatant was removed and analyzed on a Zorbax Eclipse XDB C-18 column (3.5 μm, 3 × 150 mm, 35°C, Agilent) using a linear gradient from 0 to 40% acetonitrile over 14 min with 0.1% formic acid as the aqueous mobile phase after an initial hold at 0% acetonitrile for 30 s (0.8 mL/min). Products were monitored using an Agilent G1315D diode array detector (TKL, $A_{260\ nm}$ or $A_{275\ nm}$; F-TKL, $A_{247\ nm}$; NDK-SNAC; $A_{260\ nm}$). The identity of each compound was verified using an Agilent 6130 single quadruple mass spectrometer in negative ion mode. For absolute quantification, each analyte was compared to an external standard curve. The concentration of the 2-fluoro-2-desmethyltriketide lactone (F-TKL) synthetic standard was determined by ^{19}F NMR using the ERETIC method (*55*) against an external standard of 5.00 mM 5-fluorouracil. The triketide lactone (TKL) standard was prepared enzymatically, and the 2-desmethyltriketide lactone (H-TKL) standard was synthesized as described (*56*). The concentrations of TKL and H-TKL were determined by ^{1}H NMR in D_2O using the ERETIC method against an external standard of diethylfluoromalonate (75 mM).

Enzymatic preparation of methyl- and fluorotriketide lactones from methylmalonate and fluoromalonate. Reaction mixtures (TKL, 4 mL; F-TKL, 8 mL) containing NDK-SNAC (10 mM) were prepared as described above and incubated for 18 h. Protein was removed by the addition of 70% perchloric acid (0.05 volumes) and centrifuged at 18,000 × *g* for 10 min. The supernatant was removed and extracted extensively with dichloromethane (TKL, 5 × 15 mL; F-TKL, 5 × 30 mL) and the organic layers concentrated to 5-10 mL by rotary evaporation. The residue was transferred to a silanized glass vial (Sigmacote®, Sigma-Aldrich) and 50 mM sodium bicarbonate was added (1 mL). The dichloromethane was removed from the biphasic mixture by rotary evaporation to transfer the triketide into the aqueous phase. The aqueous solution of triketide was purified on a Zorbax Eclipse XDB C-18 column (5 μm, 9.4 × 250 mm, Agilent) using a linear gradient from 0 to 27.5% methanol with 50 mM sodium phosphate, pH 4.5 over 45 min as the aqueous mobile phase (3 mL/min). Fractions containing triketide were pooled and

extracted with dichloromethane (4 × 3 volumes), and the combined organic layers were dried over magnesium sulfate and concentrated.

The TKL was purified further on a Zorbax Eclipse XDB C-18 (5 μm, 9.4 × 250 mm, Agilent) using a linear gradient from to 0 to 30% acetonitrile with 0.1% formic acid as the aqueous mobile phase over 45 min (3 mL/min) after transferring back into bicarbonate buffer as described above. Fractions containing TKL were combined and lyophilized for analysis. Due to the presence of a β-keto moiety, TKL was expected to be produced as a diastereomeric mixture, and was in fact isolated as a 100:7 mixture of (2*R*,4*S*,5*R*)-2,4-Dimethyl-3-oxo-5-hydroxy-*n*-heptanoic acid δ-lactone and its 2*S*-epimer. The observed NMR spectra are in agreement with the literature (*57*). **^{1}H NMR** (500 MHz, $CDCl_3$)**:** δ 4.66 (ddd, J=8.4, 5.4, 2.9 Hz, 2*R* H_5), 4.48 – 4.42 (m, 2*S* H_5), 3.62 (q, J=6.6 Hz, 2*R* H_2), 3.25 (d, J=7.5 Hz, 2*S* H_2), 2.83 (dd, J=7.2, 4.7 Hz, 2*S* H_4), 2.63 (qd, J=7.6, 2.9 Hz, 2*R* H_4), 1.93 – 1.82 (m, 2*R* H_{6a}), 1.65 (dqd, J=14.8, 7.6, 5.4 Hz, 2*R* H_{6b}), 1.48 (d, J=7.5 Hz, 2*S* C_2-C$\underline{H}_3$), 1.37 (d, J=6.7 Hz, 2*R* C_2-C$\underline{H}_3$), 1.16 (d, J=6.4 Hz, 2*S* C_4-C$\underline{H}_3$), 1.12 (d, J=7.5 Hz, 2*R* C_4-C$\underline{H}_3$), 1.08 (t, J=7.5 Hz, 2*R* H_7), 1.01 (t, J=7.5 Hz, 2*S* H_7). **^{13}C NMR** (226 MHz, $CDCl_3$, only the 2*R* epimer was detected)**:** δ 205.59 (C_3), 170.21 (C_1), 78.68 (C_5), 50.56 (C_2), 44.52 (C_4), 24.19 (C_6), 10.09 (C_7), 9.90 (C_4-C$\underline{H}_3$), 8.40 (C_2-C$\underline{H}_3$). **HR-ESI-MS [M-H]$^-$:** calculated for $C_9H_{13}O_3$**,** *m/z* 169.0870, found *m/z* 169.0871.

The enzymatic F-TKL was compared against an authentic synthetic standard by LC-MS, HR-ESI-MS, ^{19}F-NMR, and GC-MS (*Figure 4, Figure S13*). **^{19}F-NMR** (565 MHz, $CDCl_3$, $CFCl_3$ = 0 ppm): -171.95 (broad singlet), -210.32 (d, J = 45.8 Hz). **GC-MS:** t_R, 8.56 min; EI spectrum (*Figure S13*). **HR-ESI-MS [M-H]$^-$**: calculated for $C_8H_{10}FO_3$**,** *m/z* 173.0619, found *m/z* 173.0623.

Enzymatic preparation of F-TKL from fluoroacetate. One-pot reaction mixtures containing 200 mM HEPES, pH 7.5, TCEP (2 mM), bovine serum albumin (3 mg/mL), magnesium chloride (5 mM), fluoroacetate (10 mM), NDK–SNAC (10 mM), coenzyme A (2 mM), sodium bicarbonate (75 mM), ATP (2.5 mM), phosphoenolpyruvate (50 mM), pyruvate kinase (18 U/mL), myokinase (10 U/mL), AckA (10 μM), Pta (1 μM), ACCase (15 μM), MatB (40 μM), methylmalonyl-CoA epimerase (5 μM) and $DEBS_{Mod6}$+TE (10 μM) in a total volume of 1000 μL were incubated at 37°C for 1.5 hrs at which time sodium phosphate pH 7.5 (400 mM) was added to the reaction. The reaction was incubated at 37°C for a further 24 hrs. An aliquot (200 μL) was removed and prior to analysis, the aliquot was quenched by the addition of 70% perchloric acid (10 μL). F-TKL production was analyzed by LC-MS as described above using single ion monitoring at *m/*z 173 in negative ion mode. Telescope reaction mixtures containing 200 mM HEPES, pH 7.5, TCEP (2 mM), bovine serum albumin (3 mg/mL), magnesium chloride (5 mM),

fluoroacetate (10 mM), coenzyme A (1 mM), sodium bicarbonate (75 mM), ATP (2.5 mM), phosphoenolpyruvate (50 mM), pyruvate kinase (18 U/mL), AckA (10 μM), Pta (1 μM) and ACCase (15 μM) in a total volume of 1000 μL were incubated at 37°C for 1.5 hrs. The reaction was then spun through an Amicon spin concentrator (MWCO 3 kD) to remove proteins. 792 μL of the flow through was used to prepare a reaction with 400 mM sodium phosphate, pH 7.5, TCEP (2 mM), magnesium chloride (10 mM), NDK-SNAC (10 mM), phosphoenolpyruvate (50 mM), pyruvate kinase (18U/mL), myokinase (10 U/mL), MatB (40 μM), methylmalonyl-CoA epimerase (5 μM) and $DEBS_{Mod6}$+TE (10 μM) in a total volume of 1000 μL. The reactions were allowed to proceed for 24 h and were assayed as described for the one-pot reactions.

(2*S*,3*R*)-1-((*S*)-4-Benzyl-2-oxooxazolidin-3-yl)-2-methyl-1-oxopentan-3-yl 2-fluoroacetate (1). (*S*)-4-benzyl-3-((2*S*,3*R*)-3-hydroxy-2-methylpentanoyl)oxazolidin-2-one (171 mg, 0.585 mmol) was prepared as previously described (*54*) and combined with sodium fluoroacetate (70 mg, 0.703 mmol, 1.2 eq) and HATU (267 mg, 0.702 mmol, 1.2 eq) in a flame-dried round-bottom flask under a nitrogen atmosphere. Anhydrous THF (5.9 mL) and diisopropylethylamine (306 μL, 1.76 mmol, 3 eq) were added and the reaction was capped and stirred vigorously at room temperature for 44 h, during which time the white suspension turned orange-brown. The mixture was diluted with ethyl acetate and washed with saturated sodium bicarbonate, resulting in two clear layers. The orange-brown organic layer was washed again with saturated sodium bicarbonate, dried over $MgSO_4$, filtered through a plug of silica, and concentrated to give an orange-brown oil. The residue was purified by flash chromatography on silica (30 g) using a step gradient from 100% heptane to 25% ethyl acetate in heptane with the desired compound beginning to elute in 20% ethyl acetate. Fractions were concentrated to yield the product (173 mg, 84%) as a clear, colorless oil, R_f 0.35 (25% ethyl acetate/hexanes). **^{1}H NMR** (500 MHz, $CDCl_3$)**:** δ 7.39 – 7.16 (m, Ph-H), 5.31 (ddd, J=7.9, 5.9, 3.2 Hz, $H_{3'}$), 4.87 (d, J=47.0, CH_2F-C=O), 4.60 (dddd, J=9.8, 7.7, 3.5, 2.3 Hz, H_4), 4.31 (ddd, J=8.7, 7.7, 0.8 Hz, H_5 *pro-R*), 4.19 (dd, J=8.9, 2.3 Hz, H_5 *pro-S*), 4.09 (qd, J=6.9, 3.2 Hz, $H_{2'}$), 3.28 (dd, J=13.4, 3.5 Hz, H_{6a}), 2.78 (dd, J=13.4, 9.8 Hz, H_{6b}), 1.79 – 1.64 (m, $H_{4'}$), 1.22 (d, J=6.9 Hz, C_2-CH_3), 0.95 (t, J=7.4 Hz, $H_{5'}$). **^{13}C NMR** (151 MHz, $CDCl_3$)**:** δ 173.95 ($C_{1'}$), 168.04 (d, J=22.0 Hz, CH_2F-C=O), 153.83 (N-C=O-O), 135.41 (C_{aryl}), 129.56 (C_{aryl}), 129.07 (C_{aryl}), 127.48 (C_{aryl}), 77.44 (d, J=182.3 Hz, CH_2F-C=O) , 76.40 ($C_{3'}$), 66.58 (C_5), 55.94 (C_4), 41.00 ($C_{2'}$), 38.05 (C_6), 25.16 ($C_{4'}$), 10.15 ($C_{2'}$-CH_3), 10.04 ($C_{5'}$). **^{19}F NMR** (565 MHz, $CDCl_3$, $CFCl_3$ = 0 ppm)**:** δ -230.44 (t, J=47.0 Hz). **HR-ESI-MS $[M+Na]^+$:** calculated for $C_{18}H_{22}FNO_5Na$, *m/z* 374.1374, found *m/z* 374.1381.

Preparation of (2S,4S,5R)-2-fluoro-4-methyl-3-oxo-5-hydroxy-n-heptanoic acid δ-lactone (F-TKL). Lactonization of **1** was carried out using literature methods (*56*). **1** (160 mg, 0.455

mmol) was dried under vacuum in a pear-shaped flask then placed under nitrogen. In a flame-dried round-bottom flask, anhydrous THF (4.5 mL) and LiHMDS (1.0 M in THF, 1.366 mL, 3 eq) were combined, stirred and cooled to -78°C under nitrogen. The starting material was dissolved in anhydrous THF (3.5 mL), cooled to -78°C, and cannulated dropwise into the solution of base over 20 min. A rinse of anhydrous THF (1.5 mL) was also transferred by cannula. The reaction mixture was stirred for 3 h at -78°C and quenched by addition of saturated ammonium chloride/methanol/water (1:1:1 v/v/v, 13 mL). The mixture was then allowed to warm to room temperature while stirring. The pH of the quenched mixture was adjusted to 9 using 10 M NaOH and extracted with 3 × 40 mL ethyl acetate to remove the oxazolidinone auxiliary. The aqueous layer was adjusted to pH 2 using 12 M HCl and then extracted with 5 × 20 mL dichloromethane. The combined organic layers were concentrated to give a clear, colorless oil, which contained approximately 1 mol% starting material by ^{1}H NMR (36 mg, 45%). The product was further purified by flash chromatography on silica by washing extensively with dichloromethane (R_f < 0.05) then eluting with ethyl acetate (R_f ~ 0.4), and concentrated to yield a white, crystalline solid (13 mg, 16%). A mixture of enol (53%) and keto (47%) tautomers was observed in $CDCl_3$ (*Figure S10-11*). The keto form was almost exclusively the 2*S* diastereomer as determined by ^{1}H NOESY and molecular modeling *(Figure S12).* The doublet in the ^{19}F NMR spectrum in $CDCl_3$ at -205.96 ppm was assigned to the 2*R* keto diastereomer based on ^{1}H-^{19}F HMBC (*Figure S12C*). **^{1}H NMR** (500 MHz, $CDCl_3$)**:** δ 5.83 (d, J=45.7 Hz, *keto* H_2), 4.71 (ddd, J=8.4, 5.2, 3.0 Hz, *keto* H_5), 4.26 (ddd, J=8.8, 6.0, 3.3 Hz, *enol* H_5), 2.68 (qd, J=7.5, 3.0 Hz, *keto* H_4), 2.45 (qt, J=7.2, 3.8 Hz, *enol* H_4), 1.88 – 1.78 (m, *keto* H_{6a}), 1.75 (m, *enol* H_{6a}), 1.60 (m, *keto* H_{6b}), 1.55 – 1.44 (m, *enol* H_{6b}), 1.14 (d, J=7.5 Hz, *keto* H_8), 1.11 (d, J=7.1 Hz, *enol* H_8), 1.00 (t, J=7.4 Hz, *keto* H_7), 0.92 (t, J=7.5 Hz, *enol* H_7). ^{13}C NMR (151 MHz, $CDCl_3$): δ 198.58 (d, J=13.4 Hz, *keto* C_3), 164.15 (d, J=20.0 Hz, *keto* C_1), 162.67 (d, J=24 Hz, *enol* C_1), 156.94 (d, J=6.5 Hz, *enol* C_3), 130.00 (d, J=232.3 Hz, *enol* C_2), 89.82 (d, J=206.9 Hz, *keto* C_2), 80.27 (*enol* C_5), 77.89 (d, J=1.7 Hz, *keto* C_5), 43.97 (*keto* C_4), 35.84 (*enol* C_4), 24.15 (*keto* C_6), 23.96 (*enol* C_6), 10.38 (d, J=2.7 Hz, *enol* C_8), 10.11 (*keto* C_8), 9.93 (*keto* C_7), 9.72 (*enol* C_7). **^{19}F NMR** (565 MHz, $CDCl_3$, $CFCl_3$ = 0 ppm)**:** δ -172.36 (d, J=4.3 Hz, *enol*), -205.96 (d, J=44.9 Hz, 2*S keto*), -210.40 (d, J=45.6 Hz, 2*R keto*). **^{19}F NMR** (565 MHz, 10% D_2O, 50 mM sodium phosphate pH 4.5)**:** δ -178.66. **^{19}F NMR** (565 MHz, 15% D_2O, 85 mM Tris pH 7.5, 5-fluorouracil = -168.3 ppm)**:** δ -190.20. **GC-MS:** t_R, 8.51 min; EI spectrum (*Figure S13*). **HR-ESI-MS [M-H]$^-$:** calculated for $C_8H_{10}FO_3$**,** *m/z* 173.0619, found *m/z* 173.0617.

GC-MS analysis of F-TKL. Samples were dissolved in dichloromethane and BSTFA containing 1% trimethylsilyl chloride (Sigma-Aldrich, 0.1 volumes) was added. Samples were analyzed on a Trace GC Ultra (Thermo Scientific) coupled to a DSQII single-quadrupole mass spectrometer

using an HP-5MS column (0.25 mm × 30 m, 0.25 μM film thickness, J & W Scientific). The injection volume was 1 μL and the oven program was as follows: 75°C for 3 min, ramp to 25°C at 25°C min^{-1}, ramp to 300°C at 50 °C min^{-1}, hold for 1 min. The comparison between the synthetic and enzymatic F-TKL is shown in Figure S13.

Covalent inhibition assay for $DEBS_{Mod6}$+TE. Two triketide reaction mixtures (200 μL) were prepared as described above, one containing fluoromalonate (10 mM) and the other methylmalonate (10 mM). $DEBS_{Mod6}$+TE (10 μM) and NDK-SNAC (2.5 mM) were added to each and the reactions were incubated at 37°C for 18 h. The protein fraction was isolated from each mixture at room temperature by desalting on a Sephadex G-25 column (3 mL) using 400 mM sodium phosphate, pH 7.5. Fractions were pooled by Bradford assay and concentrated to 200 μL using Amicon Ultra spin concentrators (3 kDa MWCO). The isolated $DEBS_{Mod6}$+TE was assayed by adding TCEP (2.5 mM), methylmalonyl-CoA (1 mM) and NDK-SNAC (1 mM) to this mixture to give a final volume of 210 μL and incubating at 37°C for 3 h, then analyzed by HPLC as described above.

Triketide lactone production using $DEBS_{Mod3/6}$+TE/AT^0. All assay mixtures contained 400 mM sodium phosphate, pH 7.5, phosphoenolpyruvate (50 mM), TCEP (5 mM), magnesium chloride (10 mM), ATP (2.5 mM), pyruvate kinase (27 U/mL), myokinase (10 U/mL), methylmalonyl-CoA epimerase (5 μM), CoA (1 mM), MatB (40 μM), methyl- or fluoromalonate (20 mM) and NDK-SNAC (5 mM). When used, DszsAT (5 μM) was also added to the reaction mixture. Reactions were initiated by addition of the appropriate DEBS+TE construct (Mod6 or Mod6/AT^0, 10 μM; Mod3 and Mod3/AT^0, 5 μM in reactions containing DszsAT and 8 μM otherwise) and incubated at 37°C for 18-20 h. Aliquots were removed, quenched, processed and analyzed as described above.

Triketide lactone production using $DEBS_{Mod2}$/AT^0. All assay mixtures contained 400 mM sodium phosphate, pH 7.5, phosphoenolpyruvate (20 mM), TCEP (5 mM), magnesium chloride (5 mM), ATP (2.5 mM), pyruvate kinase (18 U/mL), myokinase (10 U/mL), methylmalonyl-CoA epimerase (5 μM), CoA (1 mM), MatB (20 μM), NDK-SNAC (500 μM) and either methylmalonate, fluoromalonate or malonate (5 mM) as appropriate. Reactions were initiated by addition of $DEBS_{Mod2}$/AT^0 (10 μM) and incubated at 37°C overnight. Aliquots were removed, quenched by addition of HCl to 1 M, then processed and analyzed as described above.

Tetraketide lactone production. All reactions contained 400 mM sodium phosphate (pH 7.5 for the 2,4-dimethyl- and 2-fluoro-4-methyl-tetraketide lactone reactions and pH 6 for the 2-

methyl-4-fluoro-tetraketide lactone reaction), glycerol (20%), phosphoenolpyruvate (20 mM), TCEP (10 mM), magnesium chloride (5 mM), ATP (2.5 mM), pyruvate kinase (18 U/mL), myokinase (10 U/mL), methylmalonyl-CoA epimerase (5 μM), MatB (20 μM), CoA (1 mM), methylmalonyl-CoA (100 μM), NDK-SNAC (1 mM) and reduced nicotinamide adenine dinucleotide phosphate (NADPH; 5 mM).

The reaction to produce 2,4-dimethyl-tetraketide lactone also contained methylmalonate (5 mM), $DEBS_{Mod2}$ (10 μM) and $DEBS_{Mod3}$+TE (2 μM). The reaction to produce 2-fluoro-4-methyl-tetraketide lactone also contained fluoromalonate (5 mM), $DEBS_{Mod2}$ (10 μM), $DEBS_{Mod3}/AT^0$ (2 μM) and DzAT (2 μM). The reaction to produce 2-methyl-4-fluoro-tetraketide lactone also contained fluoromalonate (5 mM), $DEBS_{Mod2}/AT^0$ (10 μM) and $DEBS_{Mod3}$ (2 μM).

All reactions were initialized by the addition of $DEBS_{Mod2}$ or $DEBS_{Mod2}/AT^0$ and incubated at 37°C overnight. Reactions were then saturated with sodium chloride and the aqueous layer was acidified by the addition of 0.1 volumes of 70% perchloric acid and extracted four times into 2 volumes of chloroform. The chloroform layer was concentrated by vacuum centrifugation and the tetraketide lactones were resuspended in water for analysis. Tetraketide lactones were analyzed by LC-MS using a Phenomenex Kinetex XB-C18 1.7 μm 150 x 2.1 mm column with a mobile phase of ammonium acetate (50 mM) with a gradient from 0 to 60% acetonitrile over 15 min and detected on an Agilent single quadruple mass spectrometer in negative ion mode.

ESI-MS/MS analysis of tetraketide lactones. MS/MS spectra were collected using an LTQ FT (Thermo Scientific). Negative ions were generated using ES and analyzed in linear ion trap mode. MS/MS spectra were collected with the following normalized collision energies: TKL, 26; F-TKL, 35; tetraketide lactones, 26.

Triketide lactone production under competitive conditions. For reactions with substrate regeneration, assay mixtures contained 400 mM sodium phosphate, pH 7.5, phosphoenolpyruvate (50 mM), TCEP (5 mM), magnesium chloride (10 mM), ATP (2.5 mM), pyruvate kinase (27 U/mL), myokinase (10 U/mL), methylmalonyl-CoA epimerase (5 μM), NDK-SNAC (15 mM) and $DEBS_{Mod6}$+TE (10 μM). Reactions were initiated by simultaneous addition of MatB (40 μM), fluoromalonyl-CoA (1 μM) and malonyl-CoA (1 μM) and incubated at 37°C for 18-20 h. Protein was removed by filtration through a 3 kDa NWCO membrane at 14,000 × *g* and the filtrate was analyzed by LC-MS. Standards of H-TKL and F-TKL were prepared using a mock reaction mixture (acyl-CoAs replaced by CoAs and NDK-SNAC replaced by N-acetyl cysteamine) as diluent. TKLs were quantified using single ion monitoring, H-TKL

in positive mode and F-TKL in negative mode. For reactions without substrate regeneration, assay mixtures contained 400 mM sodium phosphate, pH 7.5, TCEP (5 mM), methylmalonyl-CoA epimerase (5 μM), NDK-SNAC (3 mM) and $DEBS_{Mod6}$+TE (10 μM). Reactions were initiated by adding fluoromalonyl-CoA (1 mM) and malonyl-CoA (1 mM) simultaneously. The mixtures were incubated at 37°C for 20 h, then quenched, processed and analyzed as described above. H-TKL was monitored using an Agilent 6130 MS operating in positive ion mode, and the limit of detection was verified by spiking samples to 50 nM H-TKL using a standard solution.

^{19}F-NMR analysis of *E. coli*. LB (250 mL) containing kanamycin and chloramphenicol (50 μg/mL each) in a 1 L baffled shake flask was inoculated to OD_{600} = 0.05 with an overnight LB culture of *E. coli* BAP1 freshly co-transformed with pET28a-His_6-MatB.SCo and pTRC33-NphT7-PhaB. Cells were grown, induced, washed and resuspended at OD_{600} 90-110 as described above for F-TKL production in resting cells. To 850 μL of this cell suspension fluoromalonate (43 mM) was added and the cells were incubated at 16°C for 1 d. Cells were pelleted by centrifugation at 18,000 × *g* and the supernatant (650 μL) was removed. The volume of the supernatant was adjusted to 850 μL by addition of D_2O (extracellular fraction). Cells were resuspended in 605 μL potassium phosphate buffer, pH 7.4, and centrifuged again. The supernatant was removed and the cells were resuspended to give a final volume of 850 μL, 17% D_2O and 35 mM sodium phosphate pH 7.5. Cells were lysed by sonication and insoluble material removed by centrifugation at 18,000 × *g* for 20 min at room temperature. The supernatant was removed and acidified by addition of 0.025 volumes 70% perchloric acid. Insoluble material was removed by centrifugation at 18,000 × *g* for 20 min and the supernatant was removed. The pH was adjusted to 7 using 10 M sodium hydroxide (intracellular fraction). $CFCl_3$ was added as a chemical shift reference to both the extracellular and intracellular fractions, which were analyzed by ^{19}F NMR using the ERETIC method.

F-TKL production in *E. coli* cell lysates. TB (1 L) containing Cb and Km (50 μg/mL each) in a 2.8 L Fernbach baffled shake flask was inoculated to OD_{600} = 0.05 with an overnight TB culture of *E. coli* BAP1 freshly co-transformed with pET28a-His_6-MatB.SCo/pRSG54 or pET28a/pET16b as the empty vector control. The cultures were grown at 37°C at 250 rpm to OD_{600} = 0.6 to 0.8 at which point cultures were cooled on ice for 20 min, followed by induction of protein expression with IPTG (0.2 mM) and overnight growth at 16°C. Cell pellets were harvested by centrifugation at 9,800 × *g* for 7 min at 4ºC and stored at -80ºC. Frozen cell pellets were thawed and resuspended at 5 mL/g cell paste with sodium phosphate (500 mM, pH 7.5) and lysed by passage through a French pressure cell at 14,000 psi. The lysate was centrifuged at 15,300 × *g* for 20 min at 4°C to separate the soluble and insoluble fractions. Assay mixtures (100

μL) containing soluble cell lysate (77 μL), phosphoenolpyruvate (50 mM), TCEP (5 mM), magnesium chloride (10 mM), pyruvate kinase (27 U/mL), myokinase (10 U/mL), methylmalonyl-CoA epimerase (5 μM), fluoromalonate (10 mM), coenzyme A (500 μM), ATP (2.5 mM), and NDK-SNAC (10 mM) were incubated overnight at 37°C. Reactions were quenched by the addition of 70% perchloric acid (5 μL) and insoluble material was removed by centrifugation. Production of F-TKL was analyzed by LC-MS as described above.

F-TKL production in *E. coli* growing and resting cell culture. LB (50 mL) containing carbenicillin and kanamycin (50 μg/mL each) with or without spectinomycin (100 μg/mL) in a 250 mL baffled shake flask was inoculated to OD_{600} = 0.05 with an overnight LB culture of *E. coli* BAP1 freshly co-transformed with pET28a-His_6-MatB.SCo and the appropriate DEBS+TE plasmid, with or without pCDFDuet-DszsAT.

For F-TKL production in LB, cultures were grown at 37°C at 200 rpm to OD_{600} = 0.4 at which point cultures were cooled on ice for 10 min, followed by induction of protein expression with IPTG (0.2 mM). The cultures were grown at 30°C for 2 h following induction, at which the culture (10 mL) was transferred to a 30 mL tube. Fluoromalonate (50 mM final concentration), diethylfluoromalonate (10 mM final concentration, added as a 1 M solution in DMSO) and either NDK-SNAC (stock, 100 mM solution in 10% DMSO; final, 5 mM) or 10% DMSO were added. The cultures were grown at 30°C for 20 h. The culture supernatant was collected by centrifugation at 18,000 × *g* for 15 min and acidified by addition of HCl to a final concentration of 1 M. The acidified supernatant was then extracted with 5 × 3 volumes of dichloromethane and the combined organic layers were concentrated to 5-10 mL by rotary evaporation. The residue was transferred to a silanized glass vial (Sigmacote®, Sigma-Aldrich) and water (200 μL) was added. The dichloromethane was removed from the biphasic mixture by rotary evaporation and the aqueous solution of triketide was analyzed by LC-MS as described above.

For F-TKL production by resting cells, cultures were grown at 37°C at 200 rpm to OD_{600} = 0.8-0.9, at which point cultures were cooled on ice for 15 min, followed by induction of protein expression with IPTG (0.2 mM). The cultures were grown at 16°C for 20-24 h following induction. Cells were collected by slow centrifugation at 1,000 × *g* for 15 min at 4°C. The cells were washed once with 100 mM potassium phosphate, pH 7.4, then resuspended in the same buffer at an OD_{600} of 90-110. To 50 μL of this suspension in a 0.6 mL tube, fluoromalonate (50 mM final concentration) and NDK-SNAC (stock, 100 mM solution in 10% DMSO; final, 5 mM) were added. The cell suspensions were incubated with shaking at 16°C for 20 h. The culture supernatant was collected by centrifugation at 18,000 × *g* for 15 min and analyzed by LC-MS as

described above with no further concentration. The identity of the F-TKL produced *in vivo* was also confirmed by HR-ESI-MS. **HR-ESI-MS [M-H]$^-$:** calculated for $C_8H_{10}FO_3$**,** *m/z* 173.0619, found *m/z* 173.0619.

Supplementary Results

Table S1. (A) Strains and plasmids used for this study. (B) Oligonucleotides used for gene and plasmid construction. (C) The primer map for construction of the synthetic *nphT7* gene is also shown with non-coding portions in lowercase.

A. Strains and plasmids

Strain	*Genotype*	*Source*
BL21(de3)	F$^-$ *omp*T *gal dcm lon hsd*S_B(r_B^- m_B^-) λ(DE3 [*lac*I *lac*UV5-T7 *gene 1 ind*1 *sam*7 *nin*5])	Novagen
BAP1	F$^-$ *omp*T *gal dcm lon hsd*S_B(r_B^- m_B^-) λ(DE3 [*lac*I *lac*UV5-T7 *gene 1 ind*1 *sam*7 *nin*5]) Δ*prpRBCDE* (*sfp* (T7)*, prpE* (T7))]	(*45*)

Plasmid	*Description*	*Source*
pET16b-His_{10}-NphT7	*His_{10}-nphT7* (T7), *lacI*, Cb^r, ColE1	This study
pET16b-His_{10}-AckA.EC	*His_{10}-ackA.EC* (T7), *lacI*, Cb^r, ColE1	This study
pET16b-His_{10}-Pta.EC	*His_{10}-pta.EC* (T7), *lacI*, Cb^r, ColE1	This study
pET28a-His_6-MatB.SCo	*His_6-matB.SCo* (T7), *lacI*, Km^r, ColE1	This study
pET28a-His_6-Epi.SCo	*His_6-epi.SCo* (T7), *lacI*, Km^r, ColE1	This study
pET16b-His_{10}-THNS	*His_{10}-thns* (T7), *lacI*, Cb^r, ColE1	This study
pCDFDuet-DszsAT.SCe-MatB.SCo	*DszsAT.SCe* (T7), *matB.SCo* (T7), *lacI*, Sp^r, CloDF13	This study
pCDFDuet-ø-MatB.SCo	*matB.SCo* (T7), *lacI*, Sp^r, CloDF13	This study
pFW3	*DszsAT.SCe-His_6* (T7), *lacI,* Cb^r, ColE1	(*40*)
pTRC33-NphT7-PhaB	*nphT7.phaB* (trc), *lacIq*, Cm^r, M13	This study
pBP19	*$DEBS_{Mod2}$-His_6* (T7), *lacI,* Cb^r, ColE1	(*42*)
pSV272- His_6-MBP-$DEBS_{Mod2}$	*His_6-MBP-$DEBS_{Mod2}$* (T7), *lacI*, Km^r, ColE1	This study
pSV272-His_6-MBP-$DEBS_{Mod2}$/AT^0	*His_6-MBP-$DEBS_{Mod2}$/AT^0* (T7), *lacI*, Km^r, ColE1	This study
pAYC138	*$DEBS_{Mod6}$+TE/AT^0-His_6* (T7), *lacI,* Cb^r, ColE1	(*40*)
pRSG54	*$DEBS_{Mod6}$+TE-His_6* (T7), *lacI,* Cb^r, ColE1	(*35*)
pRSG34	*$DEBS_{Mod3}$+TE-His_6* (T7), *lacI,* Cb^r, ColE1	(*35*)
pAYC136	*$DEBS_{Mod3}$+TE/AT^0-His_6* (T7), *lacI,* Cb^r, ColE1	(*40*)
pRARE2	*ileX, argU, thrU, tyrU, glyT, thrT, argW, metT, leuW, proL, lacI,* Cm^r, p15a	Novagen
pBAD33-BirA	*birA.EC* (ara), *araC,* Cm^r, p15a	This study

B. Oligonucleotide sequences

Name	*Sequence*
nphT7 R1	aaacgaacgtcggtcatggtg
nphT7 F1	caccatgaccgacgttcgttttcgtatcattggcacgggt
nphT7 R2	gctccggcacgtacgcacccgtgccaatgatacga
nphT7 F2	gcgtacgtgccggagcgtattgtgtccaacgacgaggt
nphT7 R3	accagccggcgcacccacctcgtcgttggacacaatac

nphT7 F3	gggtgcgccggctggtgttgatgatgactggattacccgt
nphT7 R4	cgttgacgaatgccggtcttacgggtaatccagtcatcatcaac
nphT7 F4	aagaccggcattcgtcaacgtcgttgggcggcggac
nphT7 R5	tcggaggtcgcttggtcgtccgccgcccaacga
nphT7 F5	gaccaagcgacctccgacctggcaaccgcggcg
nphT7 R6	tcaacgccgcacgacccgccgcggttgccagg
nphT7 F6	ggtcgtgcggcgttgaaagcagcgggtattacgcc
nphT7 R7	gcaataaccgtcagttgctccggcgtaatacccgctgctt
nphT7 F7	ggagcaactgacggttattgcggtcgcaacgtccaccc
nphT7 R8	ggctgcggacggtccggggtggacgttgcgacc
nphT7 F8	cggaccgtccgcagccgccgacggcggcctac
nphT7 R9	cgcccagatgatgttgcacgtaggccgccgtcggc
nphT7 F9	gtgcaacatcatctgggcgcaaccggcaccgcggc
nphT7 R10	tgcacacagcgttaacatcaaatgccgcggtgccggttg
nphT7 F10	atttgatgttaacgctgtgtgcagcggcacggtttttgct
nphT7 R11	ccgccacgctggacagagcaaaaaccgtgccgc
nphT7 F11	ctgtccagcgtggcgggcacgctggtgtatcgtgg
nphT7 R12	caatgaccagtgcgtaaccgccacgatacaccagcgtgc
nphT7 F12	cggttacgcactggtcattggtgccgatctgtattcccgta
nphT7 R13	ggtccgccggattcagaatacgggaatacagatcggcac
nphT7 F13	ttctgaatccggcggaccgcaagaccgttgttctgtttgg
nphT7 R14	cgcacccgcgccgtcaccaaacagaacaacggtcttgc
nphT7 F14	tgacggcgcgggtgcgatggtgctgggtccgac
nphT7 R15	acccgtacccgtgctggtcggacccagcaccat
nphT7 F15	cagcacgggtacgggtccgatcgtccgtcgcg
nphT7 R16	caaacgtgtgcagggcaacgcgacggacgatcgg
nphT7 F16	ttgccctgcacacgtttggtggtctgaccgacctgatt
nphT7 R17	cacccgccggcacacgaatcaggtcggtcagaccac
nphT7 F17	cgtgtgccggcgggtggcagccgccaaccgct
nphT7 R18	tccaagccatccgtgtccagcggttggcggctgc
nphT7 F18	ggacacggatggcttggacgcgggtctgcaatacttcg
nphT7 R19	cctcgcgaccgtccatagcgaagtattgcagacccgcg
nphT7 F19	ctatggacggtcgcgaggtgcgtcgttttgttaccgaac
nphT7 R20	cctttaatcagttgcggcaagtgttcggtaacaaaacgacgca
nphT7 F20	acttgccgcaactgattaaaggtttcttgcacgaggcggg
nphT7 R21	gctaatatctgccgcatcgacacccgcctcgtgcaagaaa
nphT7 F21	tgtcgatgcggcagatattagccattttgtgccgcaccaagc
nphT7 R22	cgtccagcatgacaccgttcgcttggtgcggcacaaaatg
nphT7 F22	gaacggtgtcatgctggacgaggtctttggtgaactgcacc
nphT7 R23	atggtcgcacgcggcaggtgcagttcaccaaagacct
nphT7 F23	tgccgcgtgcgaccatgcaccgtaccgtcgaaacc
nphT7 R24	cgcacccgtattgccgtaggtttcgacggtacggtgc
nphT7 F24	tacggcaatacgggtgcggccagcattccgattacgatg
nphT7 R25	tgcacggactgctgcatccatcgtaatcggaatgctggc
nphT7 F25	gatgcagcagtccgtgcaggtagcttccgtccggg
nphT7 R26	gccagcaggaccagttcacccggacggaagctacc
nphT7 F26	tgaactggtcctgctggcgggttttggtggtggcatg
nphT7 R27	gcgcgaagctcgctgccatgccaccaccaaaaccc
nphT7 F27	gcagcgagcttcgcgctgatcgagtggtaagtcagcc
nphT7 R28	acccgctctagccgtcaggctgacttaccactcgatca

nphT7 F28	tgacggctagagcgggt
NphT7 G F	aatttcacacgagctcggtacccgggaggagatataccatgaccgacgttcgttttcg
NphT7 G R	gcgctgggtcattatatatctccttttcttaccactcgatcagcgcgaag
PhaB F	gaaaaggagatatataatgacccagcgcatcgcttacgtaacc
PhaB R	gcttgcatgcctgcaggtcgactctagaggatctcatgccttggctttgacgtatc
MatB.SCo F	tcgattgcacatatgtcctctctcttcccggccctct
MatB.SCo R	atcggatagctcgagtcagtcacggttcagcgcccgctt
Epi.SCo F	atcccgaatcatatgctgacgcgaatcgacca
Epi.SCo R	ttagtctggctcgagtcagtgctcaggtgactcaa
AckA.EC F	ggagatatacatatgtcgagtaagttag
AckA.EC R	attggatcctctagatcaggcagtcaggcg
Pta.EC F	attcatatgtcccgtattattatgctgatc
Pta.EC R	attctcgaggagggtaccgacgtcttac
THNS.SCo F	attcatatggcgactttgtgcagaccctcggtgtccgtcccggagc
THNS.SCo R	attactagttcatgcctgcctcaccctccgcgacacgccccgtg
pCDF-MatB.SCo F	ttagttaagtataagaaggagatatacatatgtcctctctcttcccggccctct
pCDF-MatB.SCo R	gtttctttaccagactcgagggtacctcagtcacggttcagcgcccg
pCDF-DszsAT.SCe F	gtttaactttaataaggagatataccatgaaagcatacatgtttcccgggc
pCDF-DszsAT.SCe R	cttaagcattatgcggccgcaagcttgttacgacgacgaggggctggg
MBP-M2 F	gggatcgaggaaaacctgtattttcagggcatgagcggtgacaacggcatgaccgagg
MBP-M2 R	gcttgtcgacggagctcgaattcggggatcctcagtggtggtggtggtggtgctcgagtg
MBP-M2ATnull F	gttatcggtcacgcgcagggtgaaatcgcggccgcggtggtggcgggagcgttgtcgctg
MBP-M2ATnull R	cgcgatttcaccctgcgcgtgaccgataacggccgaaggaacggcaccgcaggcacgcca

C. Primer map for synthetic *nphT7* construction

caccATGACC GACGTTCGTT TTCGTATCAT TGGCACGGGT GCGTACGTGC
gtggTACTGG CTGCAAGCAA AAGCATAGTA ACCGTGCCCA CGCATGCACG

CGGAGCGTAT TGTGTCCAAC GACGAGGTGG GTGCGCCGGC TGGTGTTGAT
GCCTCGCATA ACACAGGTTG CTGCTCCACC CACGCGGCCG ACCACAACTA

GATGACTGGA TTACCCGTAA GACCGGCATT CGTCAACGTC GTTGGGCGGC
CTACTGACCT AATGGGCATT CTGGCCGTAA GCAGTTGCAG CAACCCGCCG

GGACGACCAA GCGACCTCCG ACCTGGCAAC CGCGGCGGGT CGTGCGGCGT
CCTGCTGGTT CGCTGGAGGC TGGACCGTTG GCGCCGCCCA GCACGCCGCA

TGAAAGCAGC GGGTATTACG CCGGAGCAAC TGACGGTTAT TGCGGTCGCA
ACTTTCGTCG CCCATAATGC GGCCTCGTTG ACTGCCAATA ACGCCAGCGT

ACGTCCACCC CGGACCGTCC GCAGCCGCCG ACGGCGGCCT ACGTGCAACA
TGCAGGTGGG GCCTGGCAGG CGTCGGCGGC TGCCGCCGGA TGCACGTTGT

TCATCTGGGC GCAACCGGCA CCGCGGCATT TGATGTTAAC GCTGTGTGCA
AGTAGACCCG CGTTGGCCGT GGCGCCGTAA ACTACAATTG CGACACACGT

GCGGCACGGT TTTTGCTCTG TCCAGCGTGG CGGGCACGCT GGTGTATCGT
CGCCGTGCCA AAAACGAGAC AGGTCGCACC GCCCGTGCGA CCACATAGCA

GGCGGTTACG CACTGGTCAT TGGTGCCGAT CTGTATTCCC GTATTCTGAA
CCGCCAATGC GTGACCAGTA ACCACGGCTA GACATAAGGG CATAAGACTT

TCCGGCGGAC CGCAAGACCG TTGTTCTGTT TGGTGACGGC GCGGGTGCGA
AGGCCGCCTG GCGTTCTGGC AACAAGACAA ACCACTGCCG CGCCCACGCT

TGGTGCTGGG TCCGACCAGC ACGGGTACGG GTCCGATCGT CCGTCGCGTT
ACCACGACCC AGGCTGGTCG TGCCCATGCC CAGGCTAGCA GGCAGCGCAA

GCCCTGCACA CGTTTGGTGG TCTGACCGAC CTGATTCGTG TGCCGGCGGG
CGGGACGTGT GCAAACCACC AGACTGGCTG GACTAAGCAC ACGGCCGCCC

TGGCAGCCGC CAACCGCTGG ACACGGATGG CTTGGACGCG GGTCTGCAAT
ACCGTCGGCG GTTGGCGACC TGTGCCTACC GAACCTGCGC CCAGACGTTA

ACTTCGCTAT GGACGGTCGC GAGGTGCGTC GTTTTGTTAC CGAACACTTG
TGAAGCGATA CCTGCCAGCG CTCCACGCAG CAAAACAATG GCTTGTGAAC

CCGCAACTGA TTAAAGGTTT CTTGCACGAG GCGGGTGTCG ATGCGGCAGA
GGCGTTGACT AATTTCCAAA GAACGTGCTC CGCCCACAGC TACGCCGTCT

TATTAGCCAT TTTGTGCCGC ACCAAGCGAA CGGTGTCATG CTGGACGAGG
ATAATCGGTA AAACACGGCG TGGTTCGCTT GCCACAGTAC GACCTGCTCC

TCTTTGGTGA ACTGCACCTG CCGCGTGCGA CCATGCACCG TACCGTCGAA
AGAAACCACT TGACGTGGAC GGCGCACGCT GGTACGTGGC ATGGCAGCTT

ACCTACGGCA ATACGGGTGC GGCCAGCATT CCGATTACGA TGGATGCAGC
TGGATGCCGT TATGCCCACG CCGGTCGTAA GGCTAATGCT ACCTACGTCG

AGTCCGTGCA GGTAGCTTCC GTCCGGGTGA ACTGGTCCTG CTGGCGGGTT
TCAGGCACGT CCATCGAAGG CAGGCCCACT TGACCAGGAC GACCGCCCAA

TTGGTGGTGG CATGGCAGCG AGCTTCGCGC TGATCGAGTG GTAAgtcagc
AACCACCACC GTACCGTCGC TCGAAGCGCG ACTAGCTCAC CATTcagtcg

ctgacggcta gagcgggt
gactgccgat ctcgccca

Figure S1. SDS-PAGE gels of purified proteins. (A) Enzymes used in generation of malonyl-CoA extender units (**1**, AckA; **2**, Pta; **3**, AccA; **4**, AccB; **5**, AccC; **6**, AccD; **7**, MatB; **8**, Epi). (B) Enzymes used for chain extension reactions (**9**, THNS; **10**, NphT7;). (C) Enzymes used for polyketide production (**11**, $DEBS_{Mod2}$; **12**, $DEBS_{Mod2}/AT^{0}$; **13**, $DEBS_{Mod3}$+TE; **14**, $DEBS_{Mod3}/AT^{0}$+TE; **15**, $DEBS_{Mod6}$+TE; **16**, $DEBS_{Mod6}/AT^{0}$+TE; **17**, DszsAT).

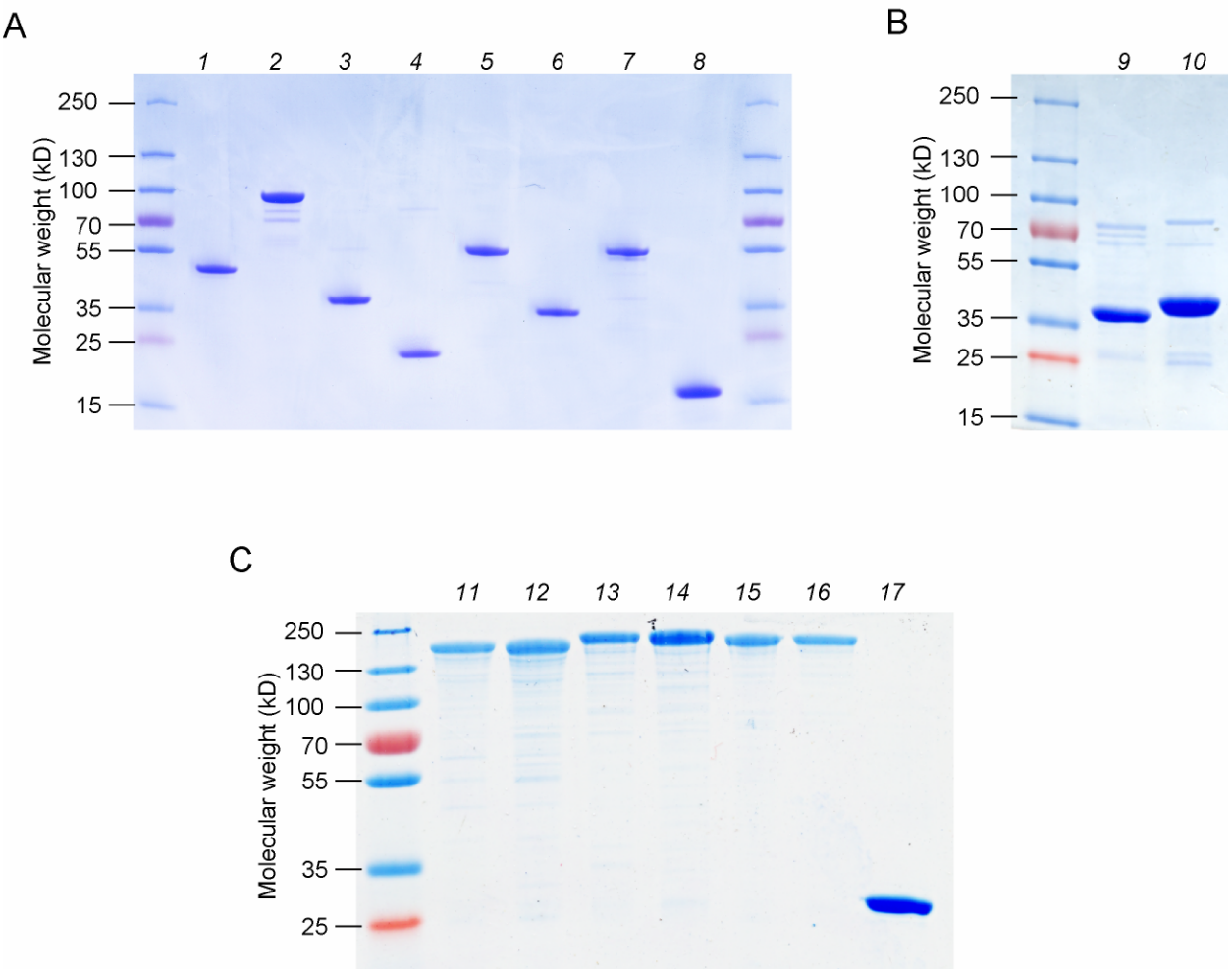

Figure S2. Formation of fluoroacetyl-CoA using AckA–Pta. (A) HPLC chromatograms monitoring fluoroacetyl-CoA formation by $A_{260\ nm}$. (B) Plot of the conversion of free CoA to fluoroacetyl-CoA. (C) Kinetic parameters for AckA and Pta measured using spectrophotometric assays reproduced from (*29*). Values are reported as the mean ± s.e. as determined from non-linear curve-fitting. Error in the k_{cat}/K_M parameter was obtained from propagation of error from the individual kinetic terms.

A

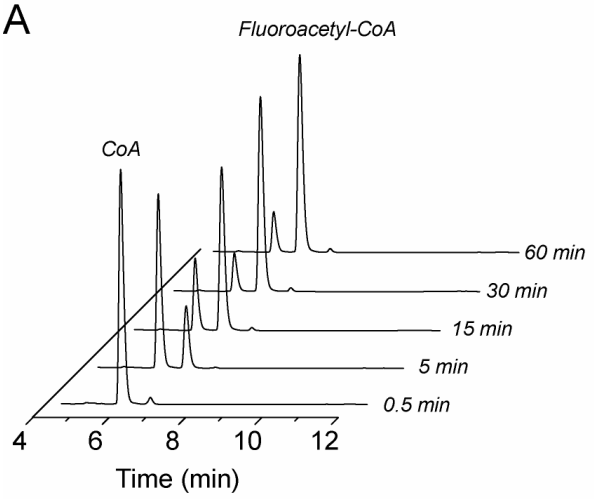

B

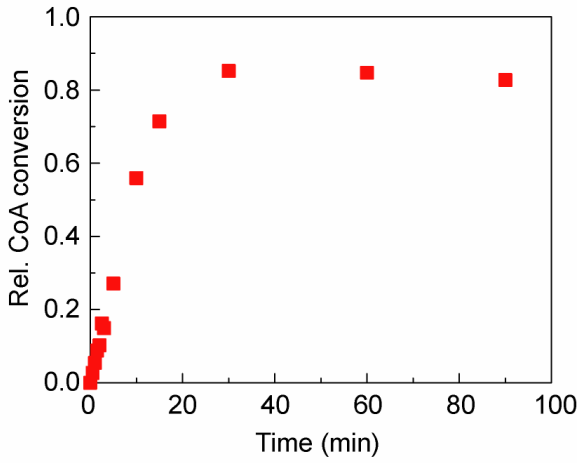

C

		k_{cat} (s^{-1})	K_M (μM)	k_{cat}/K_M ($M^{-1}s^{-1}$)
AckA	Acetate	(1.34 ± 0.03) x 10^3	(2.7 ± 0.2) x 10^4	(5.0 ± 0.4) x 10^4
	Fluoroacetate	6.7 ± 0.2	(3.3 ± 0.4) x 10^4	(2.0 ± 0.3) x 10^2
Pta	Acetyl-CoA	37 ± 1	160 ± 20	(2.3 ± 0.3) x 10^5
	Fluoroacetyl-CoA	430 ± 20	160 ± 30	(2.7 ± 0.5) x 10^6

Figure S3. Steady state kinetic analysis of MatB. (A) Malonate. (B) Methylmalonate. (C) Fluoromalonate. Values are reported as the mean ± s.e as determined from non-linear curve-fitting.

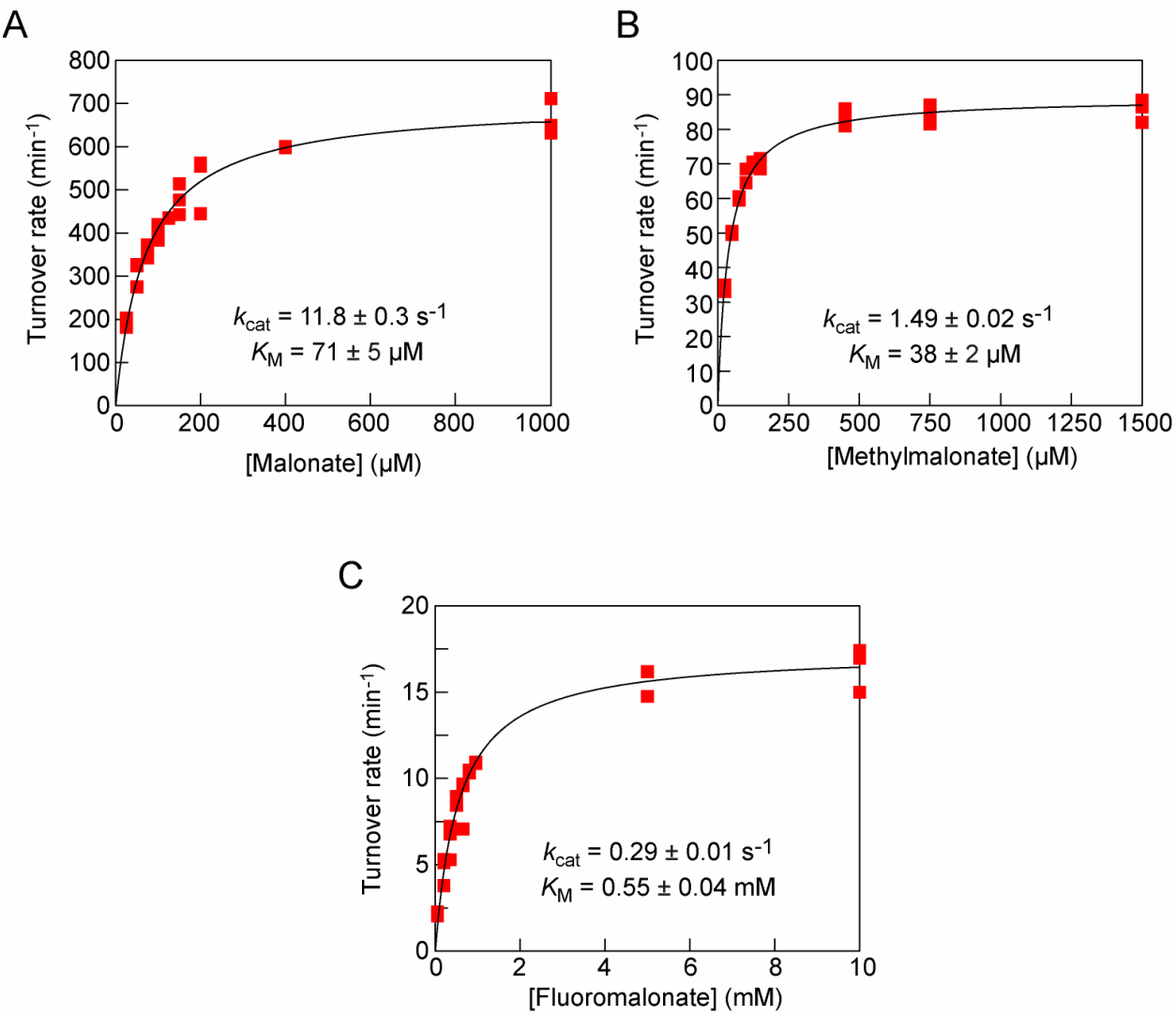

Figure S4. NMR spectra of enzymatically synthesized fluoromalonyl-CoA. (A) ^{1}H NMR. (B) ^{13}C NMR. (C) ^{19}F NMR. Spectra reflect partial (^{1}H, ^{19}F) or complete (^{13}C) H-D exchange at the fluorinated position based on incubation time.

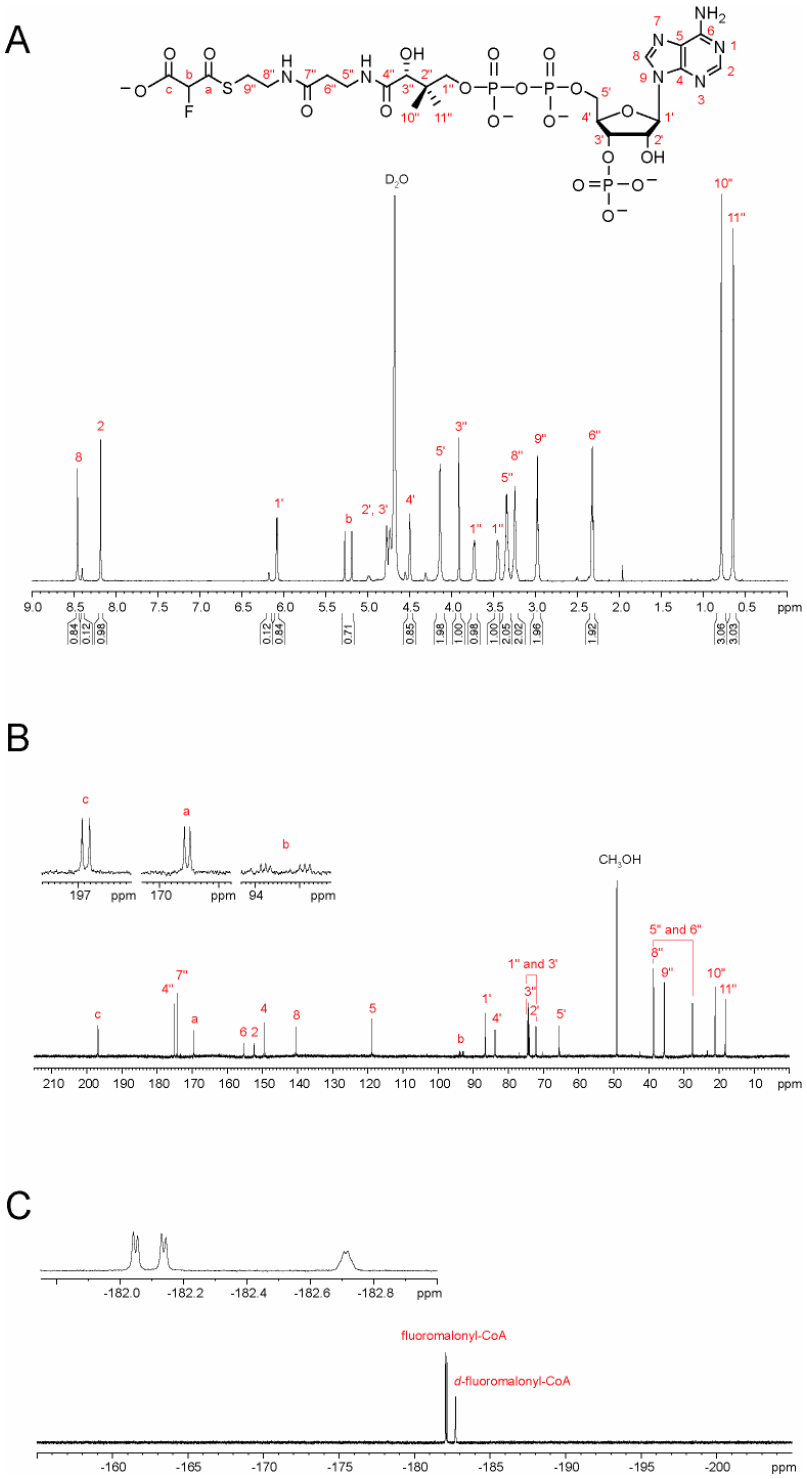

Figure S5. Efficiency of polyketide production with tetrahydroxynaphthalene synthase (THNS) using different extender regeneration systems. THNS uses only malonyl-CoA as both starter and extender unit [*10*]. All samples contained a fixed amount of malonyl- or acetyl-CoA (0.5 mM), and relative THN production was monitored at $A_{510\ nm}$. Samples with no regeneration system (**1**, **2**) were compared to those containing regeneration systems related to non-productive decarboxylation (**3**, **4**) and hydrolysis (**5**), while also providing additional substrate (**5**-**9**) *in situ*. Values are reported as the mean ± s.d. (n = 3).

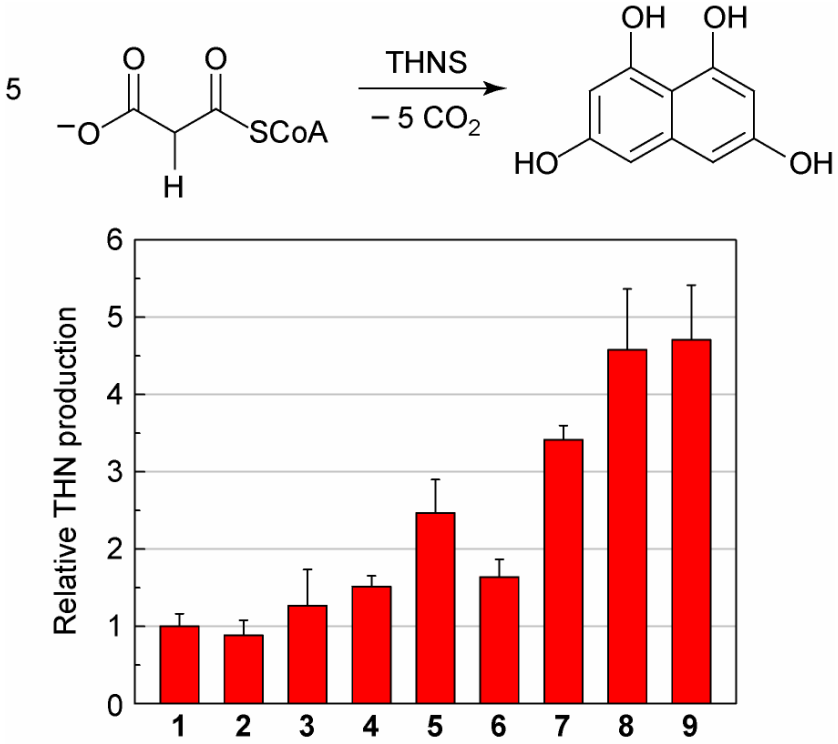

1	Malonyl-CoA
2	Malonyl-CoA, acetyl-CoA
3	Acetyl-CoA, ACCase, ATP
4	Malonyl-CoA, ACCase, ATP
5	Malonyl-CoA, MatB, malonate, ATP, myokinase
6	Acetyl-CoA, AckA/PTA, ACCase, ATP
7	Acetyl-CoA, AckA/PTA, ACCase, ATP, 1 eq acetate
8	Acetyl-CoA, AckA/PTA, ACCase, ATP, 2 eq acetate
9	Acetyl-CoA, AckA/PTA, ACCase, ATP, 20 eq acetate

Figure S6. Structural alignment of NphT7 and the $DEBS_{Mod5}$ ketosynthase (KS) domain. The NphT7 structure was predicted using Phyre2 (*58*) and based on a type III 3-oxoacyl-(acyl-carrier protein) synthase from *Burkholderia xenovorans* (PDB ID 4EFI). Despite low sequence identity (<20%), the predicted structure overlays well with the KS domain from $DEBS_{Mod5}$ (*59*). Active site residues (C119, H334 H374 (N in NphT7); DEBS numbering) are highlighted.

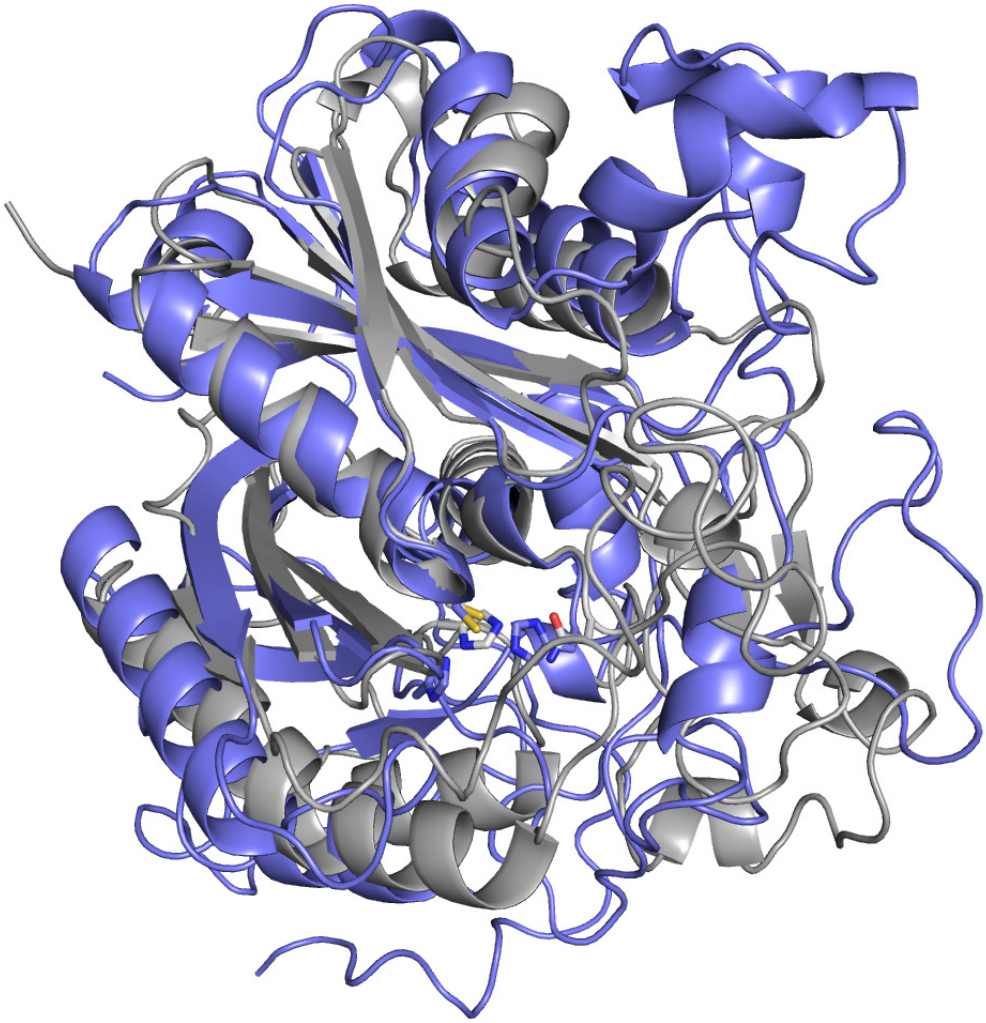

Figure S7. Characterization of enzymatically synthesized 2-fluoro-3-hydroxybutyryl-CoA. (A) LC/MS trace of 2-fluoro-3-hydroxybutyryl-CoA isolated from enzymatic reaction mixtures (*m/z* 872). (B) ^{19}F NMR spectrum indicates that both diastereomers are produced. (C) ^{1}H-^{19}F HMBC in D_2O. Based on data from other α-fluoroalcohols (*60*), the ^{19}F resonance for the anti configuration of the fluorine and hydroxyl groups should be found upfield of the syn and was assigned as the major product. If PhaB maintains is native selectivity as an *R*-specific acetoacetyl-CoA reductase, the anti product is (2*S*, 3*R*)-2-fluoro-3-hydroxybutyryl-CoA.

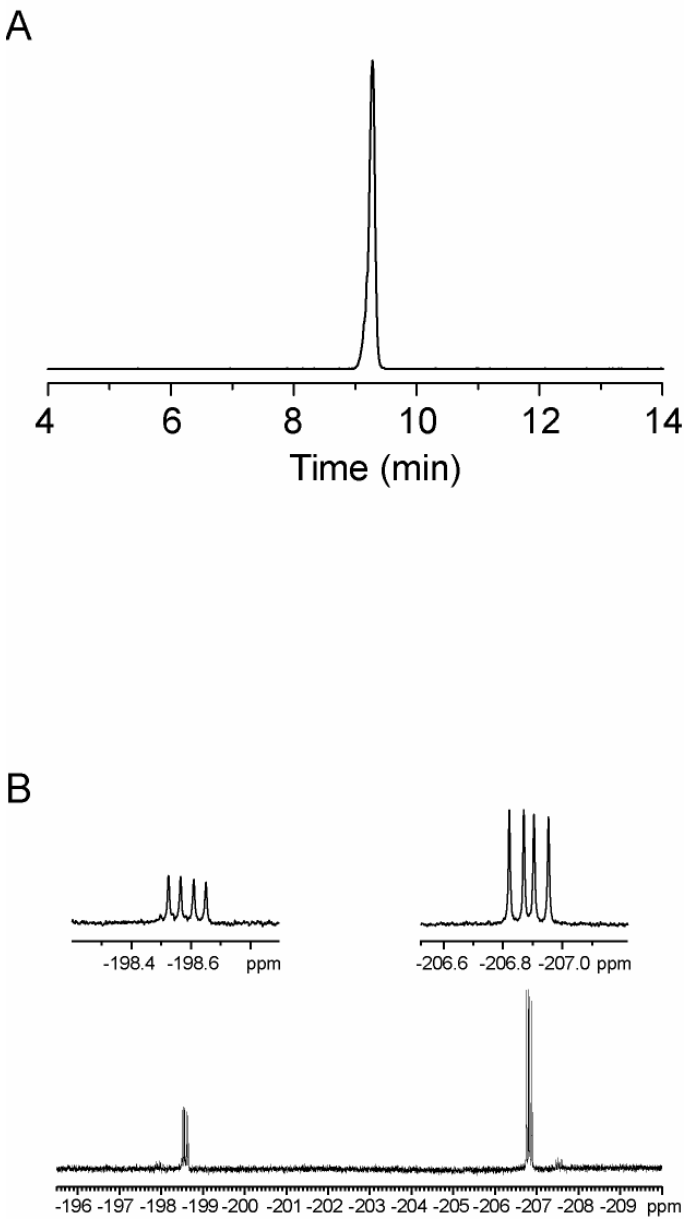

C

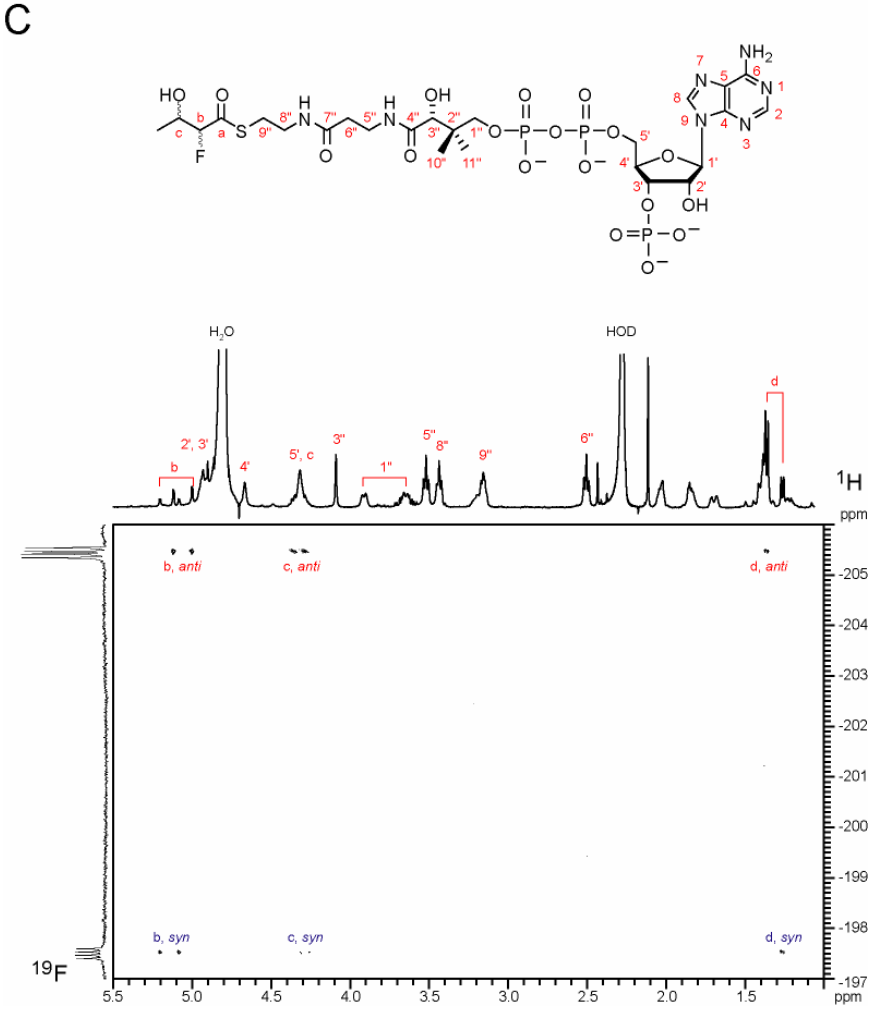
H2O
HOD
2', 3'
b
4'
5', c
3"
1"
5"
8"
9"
6"
d
1H
ppm
b, anti
c, anti
d, anti
b, syn
c, syn
d, syn
19F
-205
-204
-203
-202
-201
-200
-199
-198
-197
5.5
5.0
4.5
4.0
3.5
3.0
2.5
2.0
1.5
ppm

Figure S8. Amplification of TKL formation using MatB. All reactions contained 400 mM sodium phosphate, pH 7.5, phosphoenolpyruvate (50 mM), TCEP (5 mM), magnesium chloride (10 mM), ATP (2.5 mM), pyruvate kinase (27 U/mL), myokinase (10 U/mL), methylmalonyl-CoA epimerase (5 μM), methylmalonate (20 mM), NDK-SNAC (1 mM) and $DEBS_{Mod6}$+TE (10 μM). The source of extender unit was either methylmalonyl-CoA (0.5 – 10 mM) or MatB (40 μM) and CoA (0.5 mM). (A) Dependence of TKL formation on methylmalonyl-CoA. Data are average ± s.d. (n = 3) (B) Comparison of TKL yield with and without MatB regeneration. Values are reported as the mean ± s.d. (n = 3).

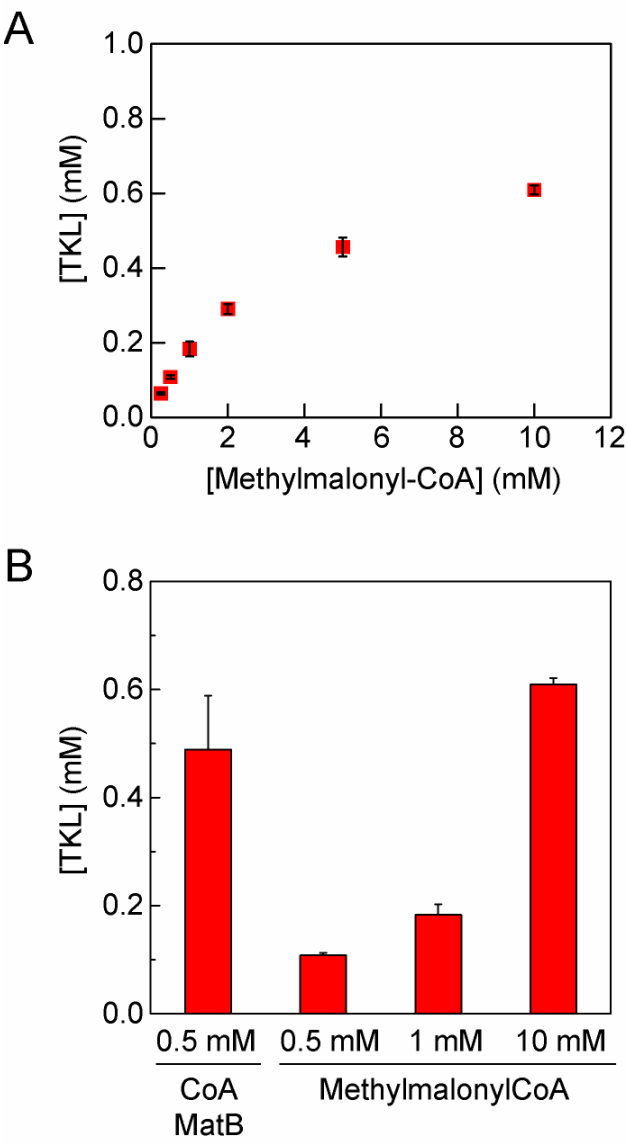

Figure S9. Time-course for TKL and F-TKL formation by $DEBS_{Mod6}$+TE with substrate regeneration. (A) LC/MS traces monitoring TKL formation (*m/z* 169) from 2.5 mM NDK-SNAC. (B) Plot of NDK-SNAC and TKL concentrations. Initial rate: 1.5 min^{-1}. (C) LC/MS traces monitoring F-TKL formation (*m/z* 173) from 10 mM NDK-SNAC. (D) Plot of NDK-SNAC and F-TKL concentrations. Initial rate: 0.14 h^{-1}. (■, NDK-SNAC; ■, TKL; ■, F-TKL)

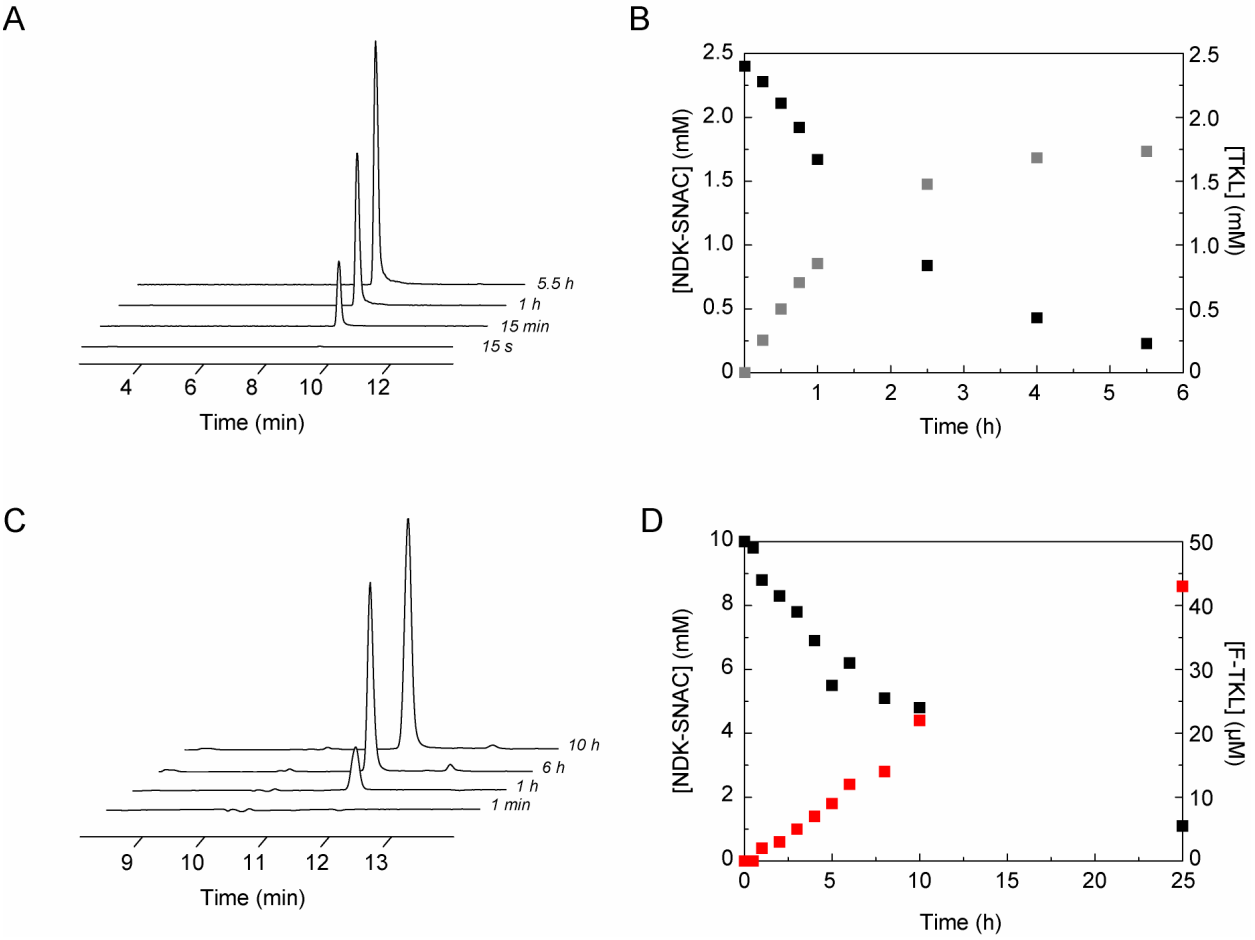

Figure S10. 1D-NMR spectra of synthetic F-TKL standard in $CDCl_3$. (A) ^{1}H NMR. (B) ^{13}C NMR. (C) ^{19}F NMR. The relative keto:enol ratio in $CDCl_3$ depends on concentration and increases with decreasing concentration.

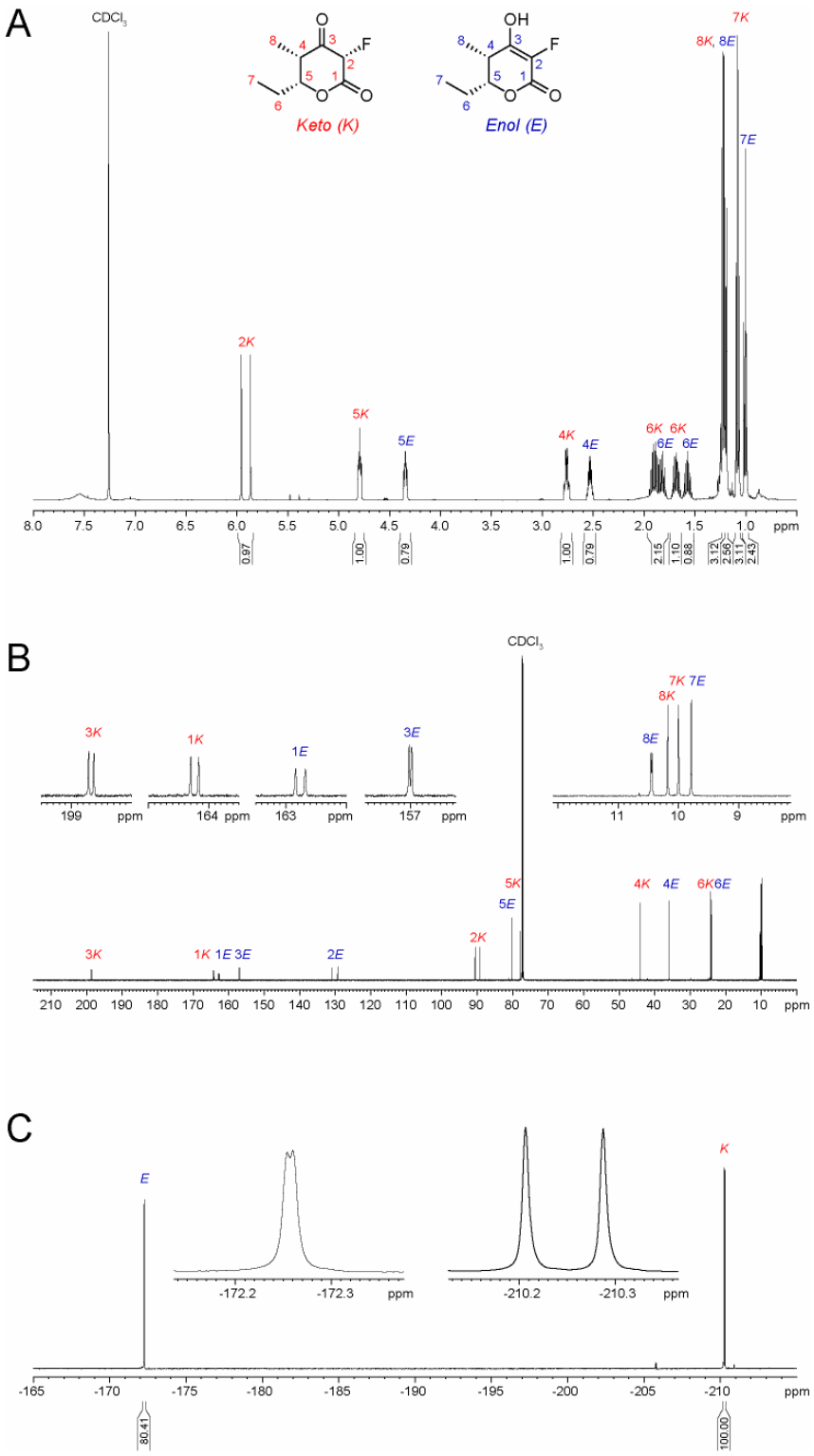

Figure S11. 2D-NMR spectra of synthetic F-TKL standard in $CDCl_3$. (A) COSY. (B) ^{1}H-^{13}C HSQC. (C) ^{1}H-^{13}C HMBC. (D) ^{1}H-^{19}F HMBC (see also *Figure S12C*).

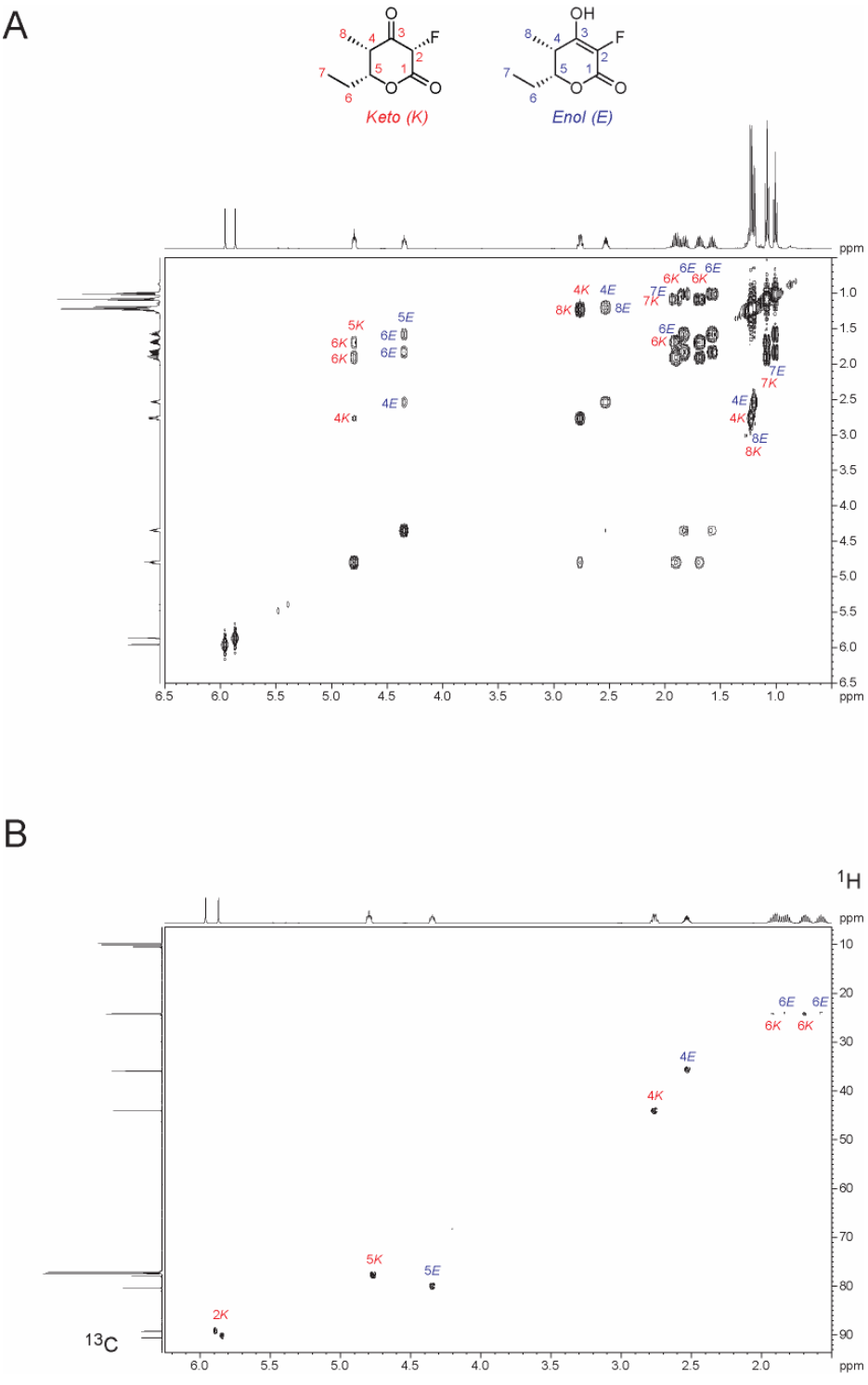

C

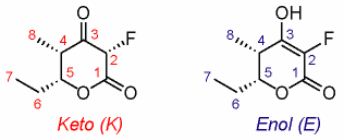

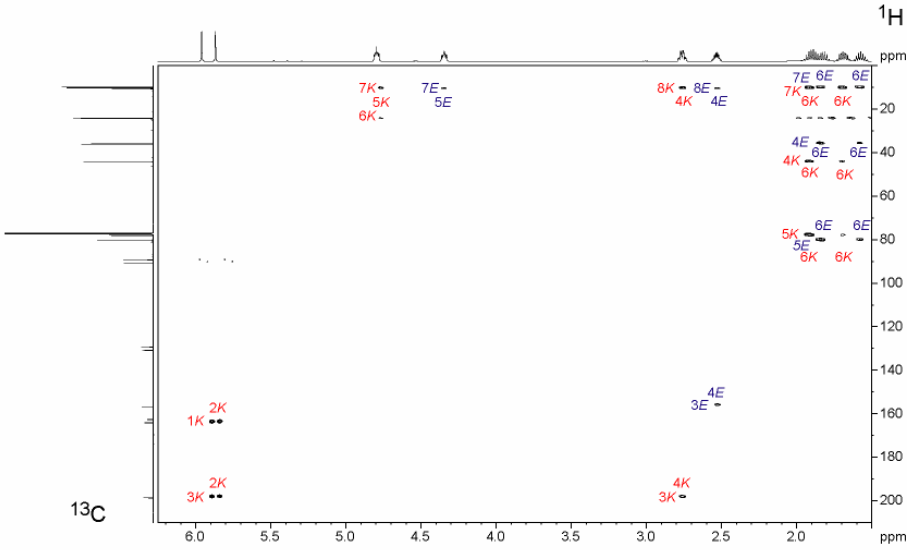

D

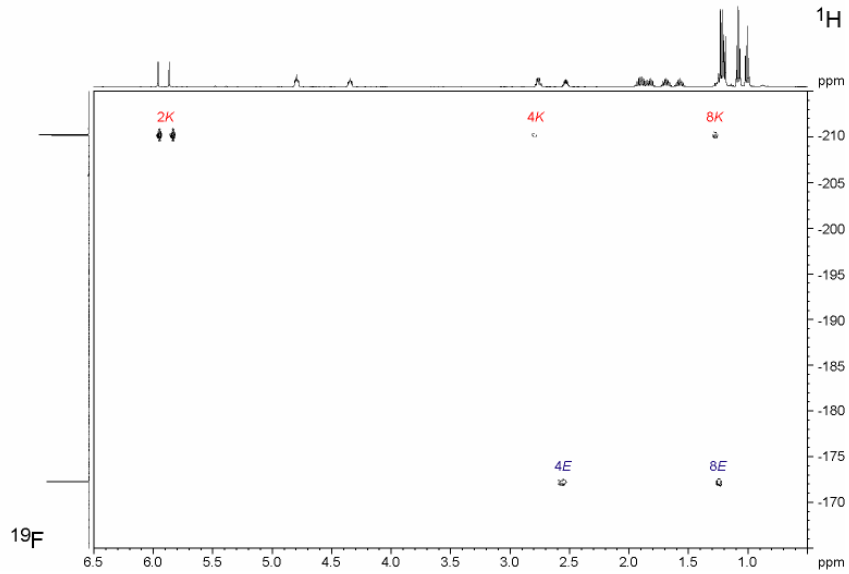

Figure S12. Stereochemical analysis for F-TKL. (A) ^{1}H NOESY spectrum of synthetic F-TKL standard in $CDCl_3$. The same ratio between epimers is observed for enzymatically produced F-TKL. (B) Molecular modeling results for F-TKL. The lowest energy conformations of the two F-TKL keto diastereomers were selected based on a conformational search (Macromodel) using Maestro 9.3 (Schrödinger, Inc). Only the 2*S* epimer would be expected to show a single NOE coupling between H_2 and H_5, as observed. (C) ^{1}H-^{19}F HMBC of keto isomer region of synthetic F-TKL standard in $CDCl_3$, showing crosspeaks for the major and minor epimers.

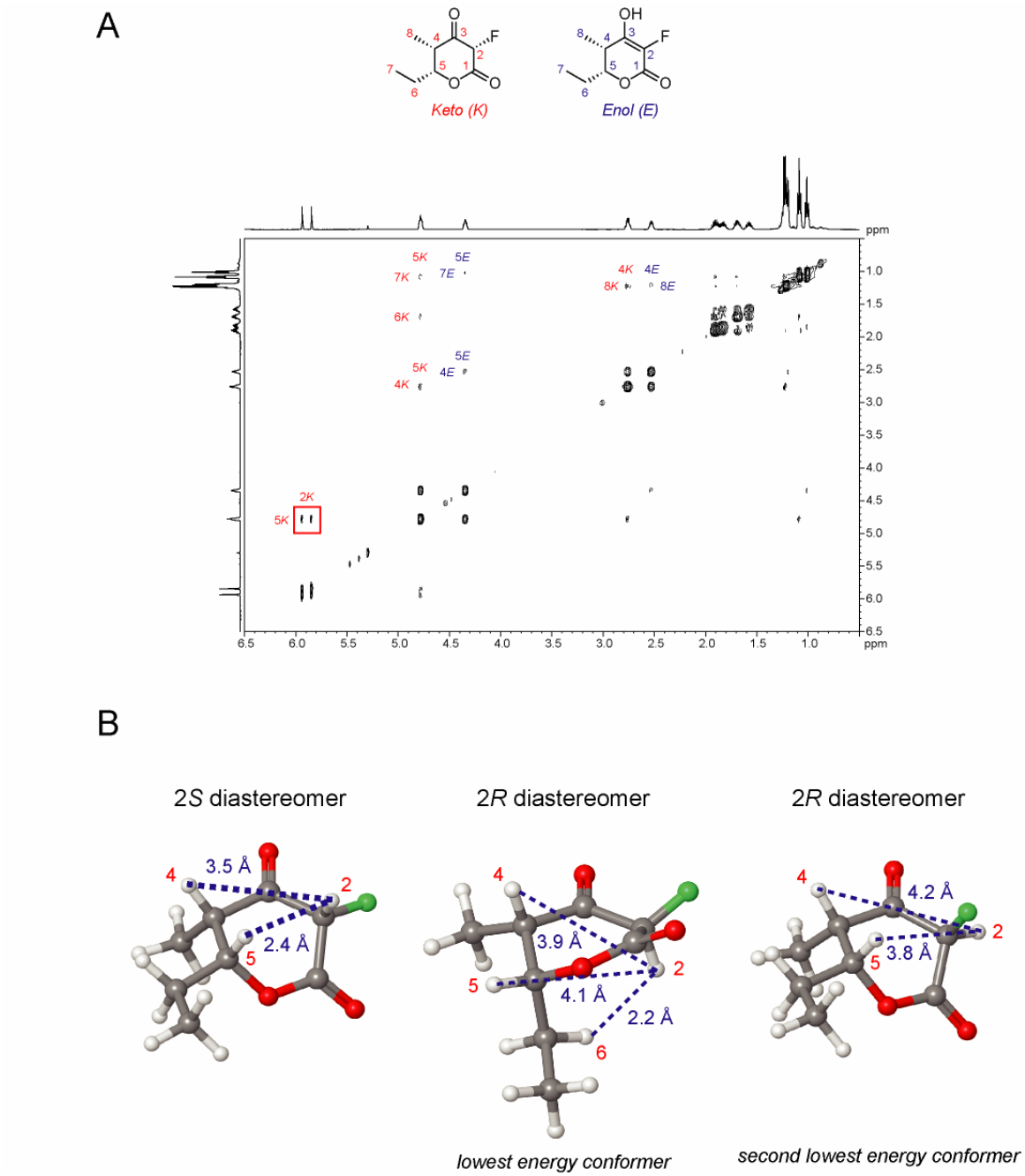

C

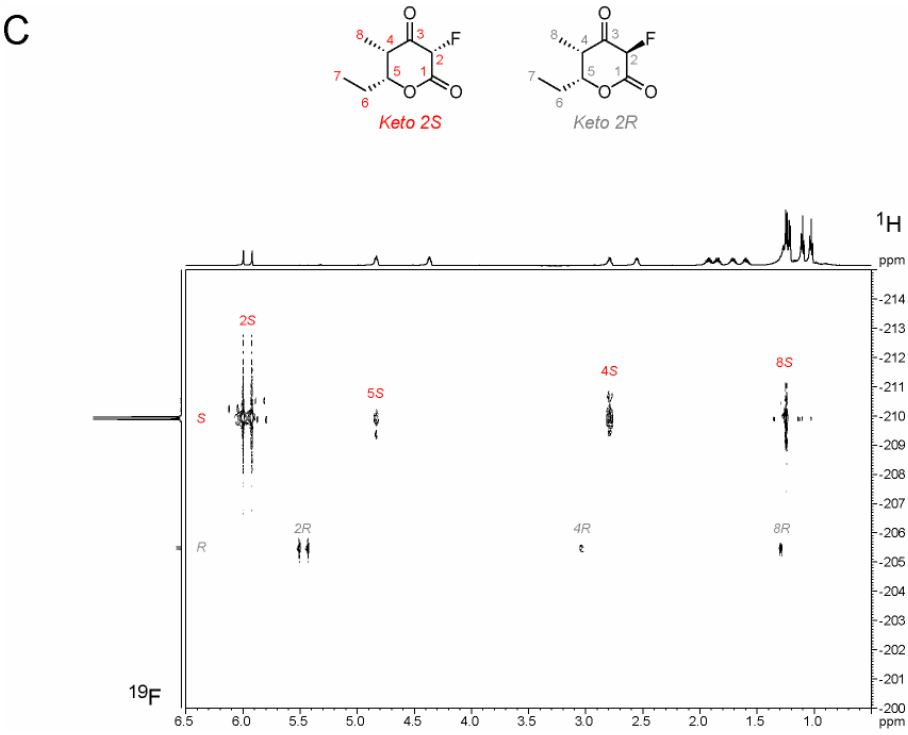
Keto 2S
Keto 2R
1H
ppm
19F
2S
5S
4S
8S
S
2R
4R
8R
R
-214
-213
-212
-211
-210
-209
-208
-207
-206
-205
-204
-203
-202
-201
-200
6.5
6.0
5.5
5.0
4.5
4.0
3.5
3.0
2.5
2.0
1.5
1.0

Figure S13. GC-MS and ^{19}F NMR comparison of enzymatic F-TKL to the authentic F-TKL synthetic standard. (A) Comparison of EI mass spectra of the standard (t_R = 8.51 min) compared to the enzymatic product (t_R = 8.56 min). (B) Comparison of ^{19}F NMR spectra in $CDCl_3$. The keto form is dominant at this concentration.

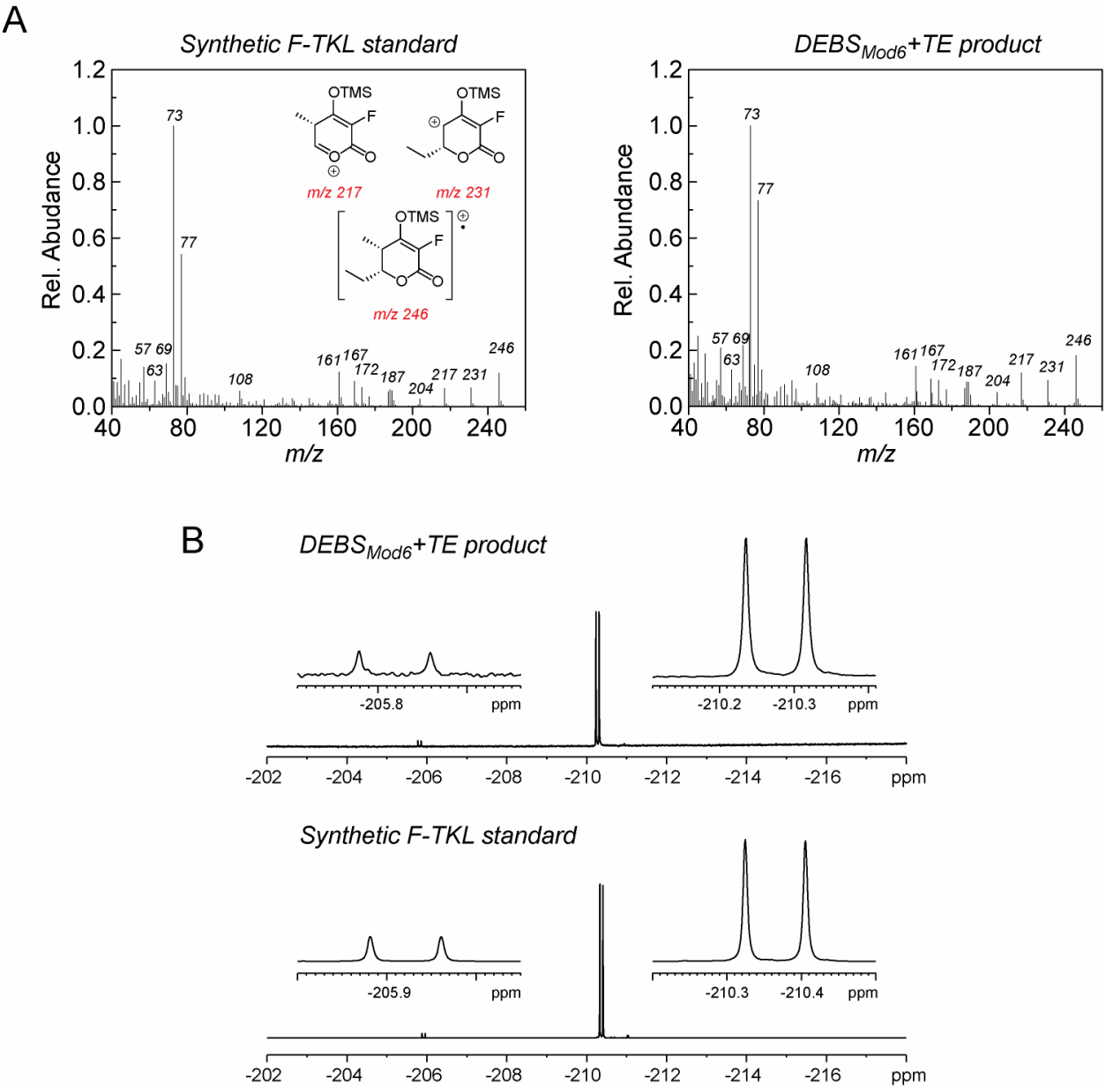

Scheme S1. Hydrolysis and regeneration reactions for F-TKL production by $DEBS_{Mod6}$+TE. Reaction scheme showing enzymes present in F-TKL forming reactions including observed non-productive hydrolysis reactions (red) and the ATP regenerating system (blue).

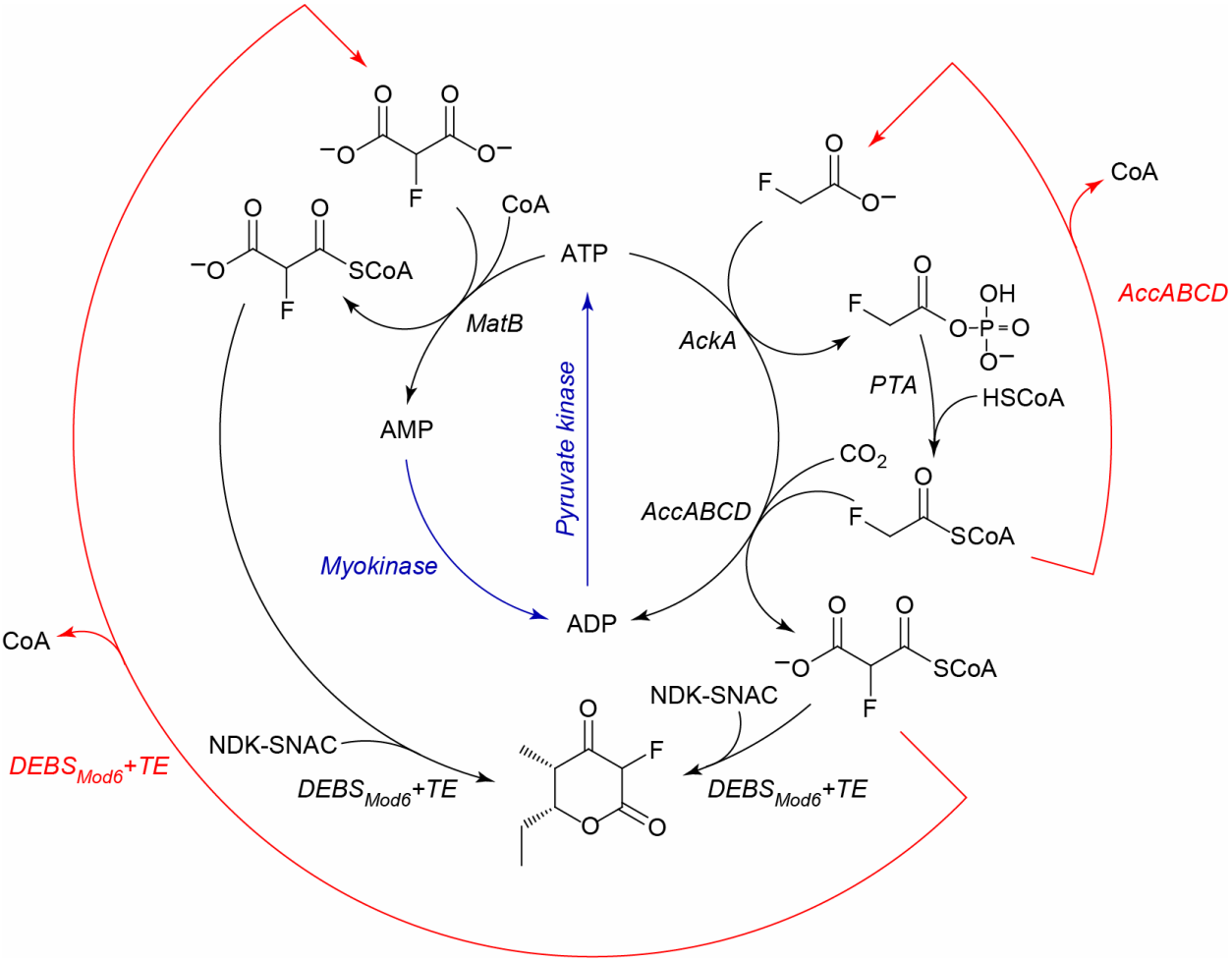

Figure S14. Test for covalent inhibition of $DEBS_{Mod6}$+TE by fluoromalonyl-CoA. $DEBS_{Mod6}$+TE was incubated for 18 h in a F-TKL or TKL reaction. The enzyme was then isolated by Sephadex G-25 and tested for its ability to produce TKL. Values are reported as the mean ± s.d. (n = 3).

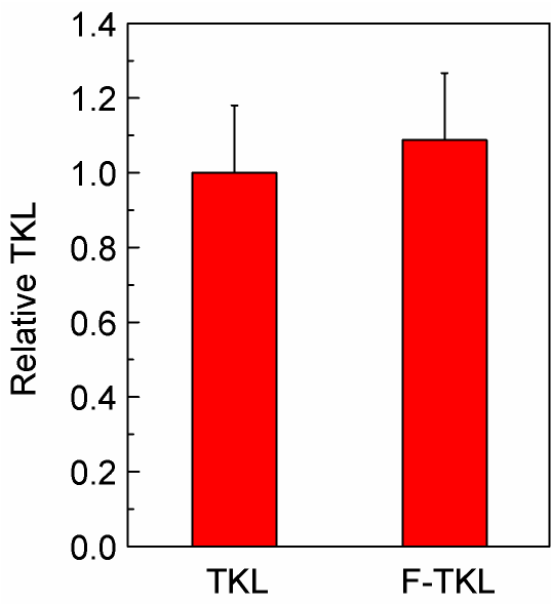

Table S2. Rates of acyl-CoA hydrolysis by $DEBS_{Mod6}$+TE. Steady-state hydrolysis rates were measured using $DEBS_{Mod6}$+TE (1 μM) and acyl-CoA (500 μM). Values are reported as the mean ± s.d. (n = 4).

	v_0 (μM min^{-1})	Relative rate
Methylmalonyl-CoA	1.36 ± 0.05	1.0
Fluoromalonyl-CoA	3.5 ± 0.3	2.6
Malonyl-CoA	6.1 ± 0.4	4.5

Figure S15. ^{19}F NMR (90% H_2O, 10% D_2O, pH 7.5) of reaction mixture for F-TKL formation by $DEBS_{Mod6}$+TE and MatB. ^{19}F NMR analysis of the reaction mixture indicates that the major pathway for loss of fluoromalonyl-CoA appears to be hydrolysis rather than unproductive decarboxylation. In addition, no detectable defluorination was observed. (IS, 5-fluorouracil, 50 μM)

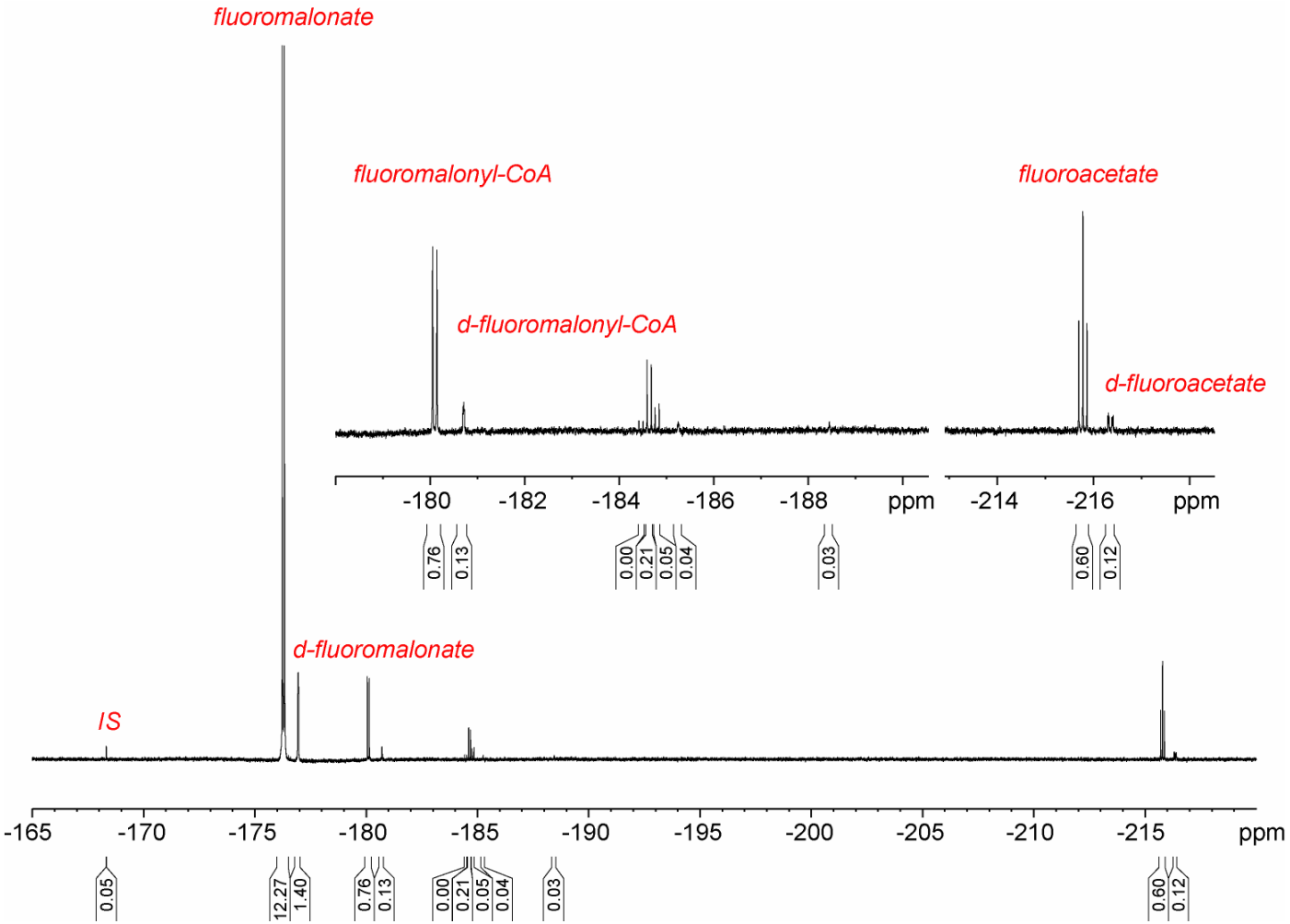

Table S3. F-TKL and H-TKL production under competitive conditions. $DEBS_{Mod6}$+TE was incubated with equimolar amounts of malonyl-CoA and fluoromalonyl-CoA (1 mM). Without substrate regeneration, no detectable H-TKL was formed (<50 nM). MatB and regeneration enzymes were then included to amplify and quantify H-TKL formation. Values are reported as the mean ± s.d. (n = 3).

Condition	[F-TKL] (nM)	[H-TKL] (nM)	[F-TKL] / [H-TKL]
No regeneration	450 ± 60	< 50	> 9
MatB regeneration	7,390 ± 520	720 ± 50	10.3 ± 0.1

Figure S16. R-TKL production *in vitro* by $DEBS_{Mod2}/AT^{0}$ under substrate regeneration conditions. When incubated overnight with NDK-SNAC (500 μM) and the methylmalonyl-CoA regenerating system, NDK-SNAC was converted quantitatively to by TKL $DEBS_{Mod2}/AT^{0}$. With the fluoromalonyl-CoA regeneration system, 82% of the NDK-SNAC was converted to F-TKL in 43% yield. With the malonyl-CoA regeneration system, 100% of the NDK-SNAC was consumed with <0.01% conversion to H-TKL. Values are reported as the mean ± s.d. (n = 3).

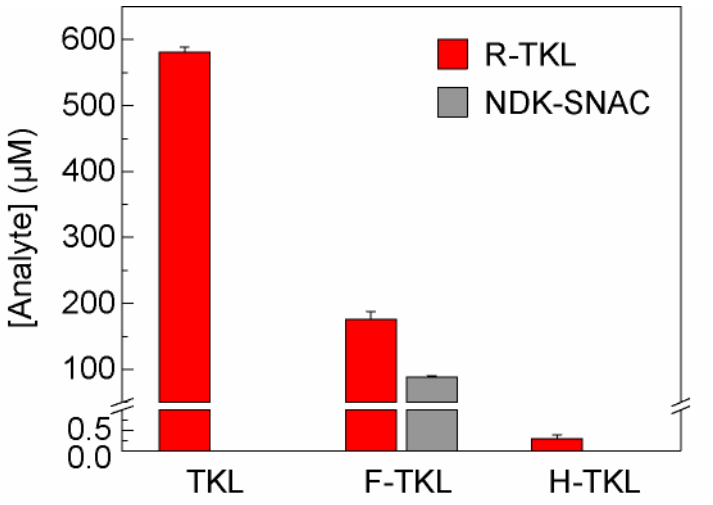

Figure S17. ESI-MS/MS data for tetraketide lactones. Authentic standards are not available for the fluorinated compounds. Both fluorinated tetraketide lactones exhibit a mass corresponding to the loss of HF (20 amu). Fragments resulting from multiple losses were not assigned structures; however, two of these fragments (**a, b**) present in the dimethyl tetraketide appear to be shifted by 4 amu in the 2-fluoro-4-methyltetraketide lactone, suggesting a fluorine for methyl substitution. Furthermore, two more fragments (**c, d**) appear to be present in the methyl form in one of the fluorinated tetraketide lactones and the fluoro form in the other regio-isomer. These fragmentation patterns suggest the 2-fluoro-4-methyl- and the 2-methyl-4-fluoro tetraketide lactones are indeed distinct regio-isomers.

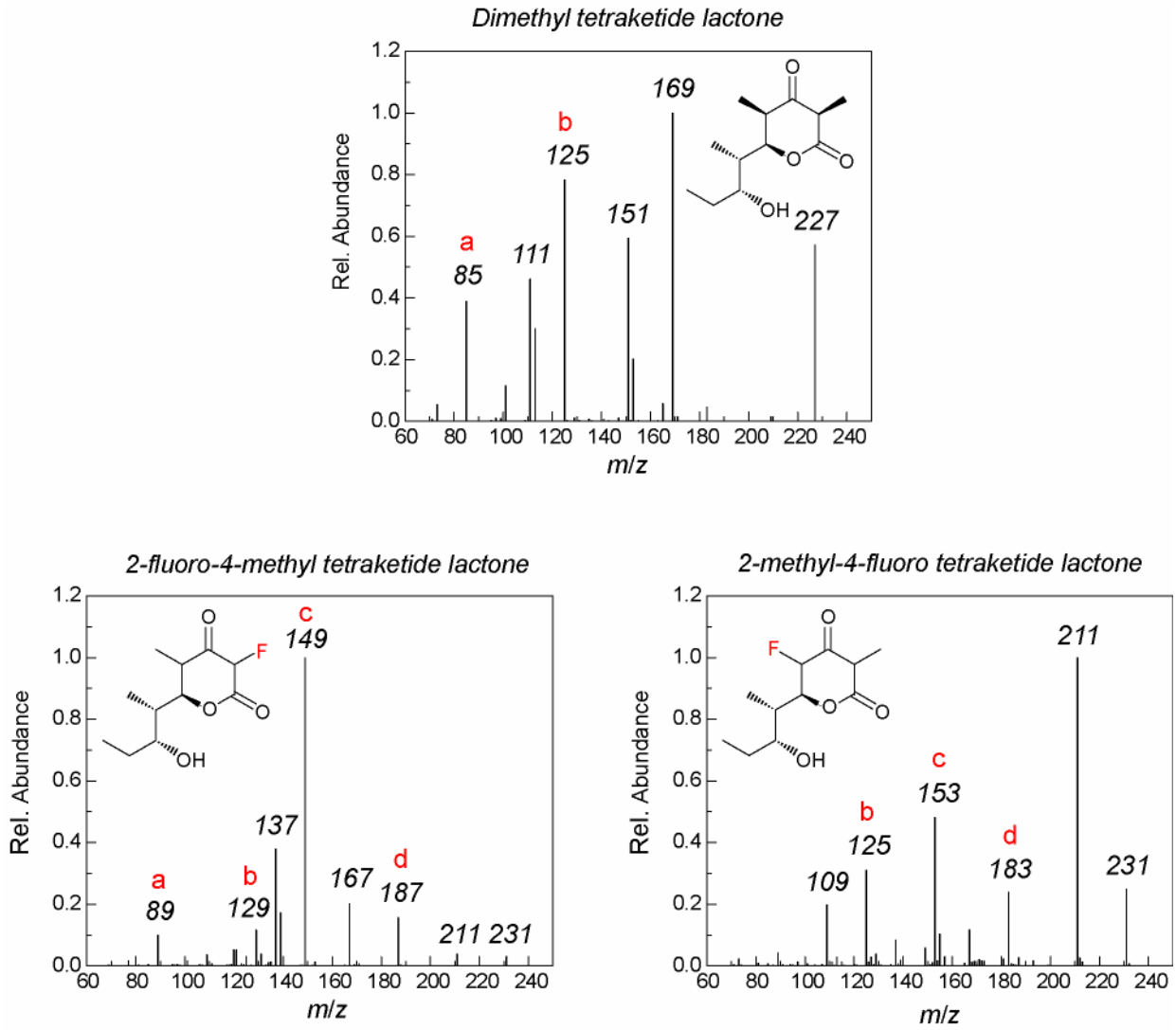

Table S4. Concentrations of extra- and intracellular organofluorines in fluorohydroxybutyrate-producing cells. Fluoromalonate (42 mM) was added to a suspension of cells expressing MatB, NphT7, and PhaB. Organofluorine concentrations were determined by ^{19}F NMR using the ERETIC method and normalized to the total suspension volume, of which the wet cell pellet constituted 33%. Chemical shifts are reported relative to the internal standard ($CFCl_3$).

		Concentration (mM)	
Species	*∂ (ppm)*	*Extracellular*	*Intracellular*
Fluoromalonate	-178.3	36.9	0.9
Fluorohydroxybutyrate	-197.4	0.2	0.1
Fluoroacetate	-217.9	1.1	0.2

Figure S18. F-TKL production *in vivo*. (A) LC/MS traces showing F-TKL formation (*m/z* 173) in *E. coli* cell lysate. (B) *In vivo* selectivity data showing F-TKL production compared to H-TKL and TKL in fluoromalonate-fed *E. coli* resting cells expressing either $DEBS_{Mod6}$+TE or $DEBS_{Mod6}$+TE/AT^0 and MatB. Bars represent mean ± s.d. (n = 3) with individual samples marked (■▲●). (C) LC/MS traces showing F-TKL formation (*m/z* 173) by *E. coli* cell culture upon feeding with NDK-SNAC.

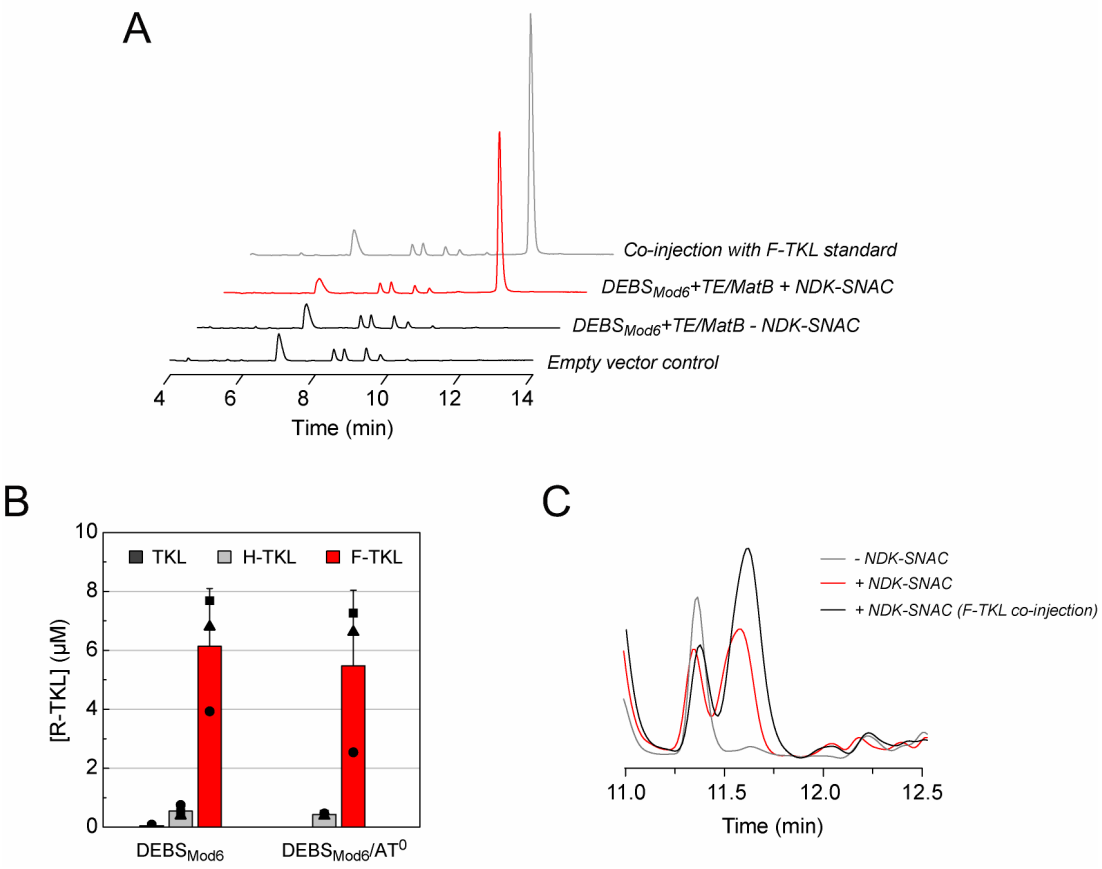

Literature Cited

1. D. K. Ro *et al.*, Production of the antimalarial drug precursor artemisinic acid in engineered yeast. *Nature* **440**, 940-943 (2006).
2. S. Atsumi, T. Hanai, J. C. Liao, Non-fermentative pathways for synthesis of branched-chain higher alcohols as biofuels. *Nature* **451**, 86-89 (2008).
3. D. E. Cane, C. T. Walsh, C. Khosla, Harnessing the biosynthetic code: Combinations, permutations, and mutations. *Science* **282**, 63-68 (1998).
4. A. M. Weeks, M. C. Y. Chang, Constructing *de novo* biosynthetic pathways for chemical synthesis inside living cells. *Biochemistry* **50**, 5404-5418 (2011).
5. K. Müller, C. Faeh, F. Diederich, Fluorine in pharmaceuticals: Looking beyond intuition. *Science* **317**, 1881-1886 (2007).
6. D. O'Hagan, Understanding organofluorine chemistry. An introduction to the C-F bond. *Chem. Soc. Rev.* **37**, 308-319 (2008).
7. T. Furuya, A. S. Kamlet, T. Ritter, Catalysis for fluorination and trifluoromethylation. *Nature* **473**, 470-477 (2011).
8. N. D. Ball, M. S. Sanford, Synthesis and reactivity of a mono-σ-aryl palladium(IV) fluoride complex. *J. Am. Chem. Soc.* **131**, 3796-3797 (2009).
9. D. A. Watson *et al.*, Formation of ArF from LPdAr(F): Catalytic conversion of aryl triflates to aryl fluorides. *Science* **325**, 1661-1664 (2009).
10. V. Rauniyar, A. D. Lackner, G. L. Hamilton, F. D. Toste, Asymmetric electrophilic fluorination using an anionic chiral phase-transfer catalyst. *Science* **334**, 1681-1684 (2011).
11. E. Lee *et al.*, A fluoride-derived electrophilic late-stage fluorination reagent for PET imaging. *Science* **334**, 639-642 (2011).
12. C. Dong *et al.*, Crystal structure and mechanism of a bacterial fluorinating enzyme. *Nature* **427**, 561-565 (2004).
13. D. O'Hagan, Recent developments on the fluorinase from *Streptomyces cattleya*. *J. Fluorine Chem.* **127**, 1479-1483 (2006).
14. A. Rivkin, K. Biswas, T.-C. Chou, S. J. Danishefsky, On the introduction of a trifluoromethyl substituent in the epothilone setting: Chemical issues related to ring forming olefin metathesis and earliest biological findings. *Org. Lett.* **4**, 4081-4084 (2002).
15. J.-P. Bégué, D. Bonnet-Delpon, Recent advances (1995-2005) in fluorinated pharmaceuticals based on natural products. *J. Fluorine Chem.* **127**, 992-1012 (2006).
16. B. Llano-Sotelo *et al.*, Binding and action of CEM-101, a new fluoroketolide antibiotic that inhibits protein synthesis. *Antimicrob. Agents Chemother.* **54**, 4961-4970 (2010).
17. S. Mo *et al.*, Biosynthesis of the allylmalonyl-CoA extender unit for the FK506 polyketide synthase proceeds through a dedicated polyketide synthase and facilitates the mutasynthesis of analogues. *J. Am. Chem. Soc.* **133**, 976-985 (2010).

18. W. Runguphan, J. J. Maresh, S. E. O'Connor, Silencing of tryptamine biosynthesis for production of nonnatural alkaloids in plant culture. *Proc. Natl. Acad. Sci. U.S.A.* **106**, 13673-13678 (2009).

19. R. J. M. Goss *et al.*, An expeditious route to fluorinated rapamycin analogues by utilising mutasynthesis. *ChemBioChem* **11**, 698-702 (2010).

20. J. Staunton, K. J. Weissman, Polyketide biosynthesis: A millennium review. *Nat. Prod. Rep.* **18**, 380-416 (2001).

21. R. Croteau, T. M. Kutchan, N. G. Lewis, in *Biochemistry and molecular biology of plants* R. B. Buchanan, W. Gruissem, R. Jones, Eds. (ASPB, Rockville, MD, 2000) pp. 1250-1318.

22. Y. A. Chan, A. M. Podevels, B. M. Kevany, M. G. Thomas, Biosynthesis of polyketide synthase extender units. *Nat. Prod. Rep.* **26**, 90-114 (2009).

23. R. McDaniel *et al.*, Multiple genetic modifications of the erythromycin polyketide synthase to produce a library of novel "unnatural" natural products. *Proc. Natl. Acad. Sci. U.S.A.* **96**, 1846-1851 (1999).

24. U. Sundermann *et al.*, Enzyme-directed mutasynthesis: A combined experimental and theoretical approach to substrate recognition of a polyketide synthase. *ACS Chem. Biol.* **8**, 443-450 (2012).

25. I. Koryakina, J. B. McArthur, M. M. Draelos, G. J. Williams, Promiscuity of a modular polyketide synthase towards natural and non-natural extender units. *Org. Biomol. Chem.*, 4449-4458 (2013).

26. A. Eustaquio, D. O'Hagan, B. Moore, Engineering fluorometabolite production: Fluorinase expression in *Salinispora tropica* yields fluorosalinosporamide. *J. Nat. Prod.* **73**, 378-382 (2010).

27. J. C. Powers, J. L. Asgian, Ö. D. Ekici, K. E. James, Irreversible inhibitors of serine, cysteine, and threonine proteases. *Chem. Rev.* **102**, 4639-4750 (2002).

28. T. D. K. Brown, M. C. Jones-Mortimer, H. L. Kornberg, The enzymic interconversion of acetate and acetyl-coenzyme A in *Escherichia coli*. *J. Gen. Microbiol.* **102**, 327-336 (1977).

29. M. C. Walker, M. Wen, A. M. Weeks, M. C. Y. Chang, Temporal and fluoride control of secondary metabolism regulates cellular organofluorine biosynthesis. *ACS Chem. Biol.*, 1576–1585 (2012).

30. A. J. Hughes, A. Keatinge-Clay, Enzymatic extender unit generation for *in vitro* polyketide synthase reactions: Structural and functional showcasing of *Streptomyces coelicolor* MatB. *Chem. Biol.* **18**, 165-176 (2011).

31. M. Izumikawa *et al.*, Expression and characterization of the type III polyketide synthase 1,3,6,8-tetrahydroxynaphthalene synthase from *Streptomyces coelicolor* A3(2). *J. Ind. Microbiol. Biot.* **30**, 510-515 (2003).

32. E. Okamura, T. Tomita, R. Sawa, M. Nishiyama, T. Kuzuyama, Unprecedented acetoacetyl-coenzyme A synthesizing enzyme of the thiolase superfamily involved in the mevalonate pathway. *Proc.Natl. Acad. Sci. U.S.A* **107**, 11265 (2010).

33. A. P. Siskos *et al.*, Molecular basis of Celmer's rules: Stereochemistry of catalysis by isolated ketoreductase domains from modular polyketide synthases. *Chem. Biol.* **12**, 1145-1153 (2005).

34. C. Khosla, Y. Tang, A. Y. Chen, N. A. Schnarr, D. E. Cane, Structure and mechanism of the 6-deoxyerythronolide B synthase. *Annu. Rev. Biochem.* **76**, 195-221 (2007).

35. R. S. Gokhale, S. Y. Tsuji, D. E. Cane, C. Khosla, Dissecting and exploiting intermodular communication in polyketide synthases. *Science* **284**, 482-485 (1999).

36. N. Wu, F. Kudo, D. E. Cane, C. Khosla, Analysis of the molecular recognition features of individual modules derived from the erythromycin polyketide synthase. *J. Am. Chem. Soc.* **122**, 4847-4852 (2000).

37. S. A. Bonnett *et al.*, Acyl-CoA subunit selectivity in the pikromycin polyketide synthase PikAIV: Steady-state kinetics and active-site occupancy analysis by FTICR-MS. *Chem. Biol.* **18**, 1075-1081 (2011).

38. G. F. Liou, J. Lau, D. E. Cane, C. Khosla, Quantitative analysis of loading and extender acyltransferases of modular polyketide synthases *Biochemistry* **42**, 200-207 (2002).

39. P. Kumar, A. T. Koppisch, D. E. Cane, C. Khosla, Enhancing the modularity of the modular polyketide synthases: Transacylation in modular polyketide synthases catalyzed by malonyl-CoA:ACP transacylase. *J. Am. Chem. Soc.* **125**, 14307-14312 (2003).

40. F. T. Wong, A. Y. Chen, D. E. Cane, C. Khosla, Protein-protein recognition between acyltransferases and acyl carrier proteins in multimodular polyketide synthases. *Biochemistry* **49**, 95-102 (2009).

41. F. T. Wong, X. Jin, I. I. Mathews, D. E. Cane, C. Khosla, Structure and mechanism of the trans-acting acyltransferase from the disorazole synthase. *Biochemistry* **50**, 6539-6548 (2011).

42. S. Y. Tsuji, D. E. Cane, C. Khosla, Selective protein-protein interactions direct channeling of intermediates between polyketide synthase modules. *Biochemistry* **40**, 2326-2331 (2001).

43. B. D. Bennett *et al.*, Absolute metabolite concentrations and implied enzyme active site occupancy in *Escherichia coli*. *Nat. Chem. Biol.* **5**, 593-599 (2009).

44. T. Haller, T. Buckel, J. Rétey, J. A. Gerlt, Discovering new enzymes and metabolic pathways: Conversion of succinate to propionate by *Escherichia coli*. *Biochemistry* **39**, 4622-4629 (2000).

45. B. A. Pfeifer, S. J. Admiraal, H. Gramajo, D. E. Cane, C. Khosla, Biosynthesis of complex polyketides in a metabolically engineered strain of *E. coli*. *Science* **291**, 1790-1792 (2001).

46. J. M. Rouillard *et al.*, Gene2Oligo: Oligonucleotide design for *in vitro* gene synthesis. *Nucleic Acids Res.* **32**, W176-W180 (2004).

47. D. G. Gibson *et al.*, Enzymatic assembly of DNA molecules up to several hundred kilobases. *Nat. Methods* **6**, 343-345 (2009).

48. B. B. Bond-Watts, R. J. Bellerose, M. C. Y. Chang, Enzyme mechanism as a kinetic control element for designing synthetic biofuel pathways. *Nat. Chem. Biol.* **7**, 222-227 (2011).

49. P. Kumar, C. Khosla, Y. Tang, Manipulation and analysis of polyketide synthases. *Method. Enzymol.*, 269-293 (2004).

50. V. Theodorou, K. Skobridis, A. G. Tzakos, V. Ragoussis, A simple method for the alkaline hydrolysis of esters. *Tetraherdon Lett.* **48**, 8230-8233 (2007).

51. J. R. Williamson, B. E. Corkey, Assays of intermediates of the citric acid cycle and related compounds by fluorometric enzyme methods. *Method. Enzymol.*, 434-513 (1969).

52. F. Huang *et al.*, The gene cluster for fluorometabolite biosynthesis in *Streptomyces cattleya*: A thioesterase confers resistance to fluoroacetyl-coenzyme A. *Chem. Biol.* **13**, 475-484 (2006).

53. N. Funa *et al.*, A new pathway for polyketide synthesis in microorganisms. *Nature* **400**, 897-899 (1999).

54. D. E. Cane, W. Tan, W. R. Ott, Nargenicin biosynthesis. Incorporation of polyketide chain elongation intermediates and support for a proposed intramolecular Diels-Alder cyclization. *J. Am. Chem. Soc.* **115**, 527-535 (1993).

55. S. Akoka, L. Barantin, M. Trierweiler, Concentration measurement by proton NMR using the ERETIC method. *Anal. Chem.* **71**, 2554-2557 (1999).

56. K. Hinterding, S. Singhanat, L. Oberer, Stereoselective synthesis of polyketide fragments using a novel intramolecular Claisen-like condensation/reduction sequence. *Tetrahedron lett.* **42**, 8463-8465 (2001).

57. G. Luo, R. Pieper, A. Rosa, C. Khosla, D. E. Cane, Erythromycin biosynthesis: Exploiting the catalytic versatility of the modular polyketide synthase. *Bioorg. Med. Chem.* **4**, 995-999 (1996).

58. L. A. Kelley, M. J. E. Sternberg, Protein structure prediction on the Web: A case study using the Phyre server. *Nat. Prot.* **4**, 363-371 (2009).

59. Y. Tang, C.-Y. Kim, I. I. Mathews, D. E. Cane, C. Khosla, The 2.7 Å crystal structure of a 194-kDa homodimeric fragment of the 6-deoxyerythronolide B synthase. *Proc. Nat. Ac. Sc. U.S.A.* **103**, 11124-11129 (2006).

60. P. K. Mohanta, T. A. Davis, J. R. Gooch, R. A. Flowers, Chelation-controlled diastereoselective reduction of α-fluoroketones. *J. Am. Chem. Soc.* **127**, 11896-11897 (2005).